Seeing Analyticity in Spin and Level Repulsion in Collider Experiments

Hao Chen (MIT)

based on [2506.06431] + upcoming work

with Cyuan-Han Chang (Chicago U.), David Simmons-Duffin (Caltech), HuaXing Zhu (Peking U.)

New Frontiers of Quantum Field and Gravity

January 12, 2026

Perturbation Theory in QM

Hamiltonian: $H = H_0 + \underbrace{\lambda V}_{\text{perturbation}}$ ⟶ Goal: solving equation $H|\Psi_n\rangle = E_n|\Psi_n\rangle$

Hilbert space: $H_0|n\rangle = E_n^{(0)}|n\rangle$ [assume no degeneracy]

Perturbative expansion:

$$E_n(\lambda) = E_n^{(0)} + \lambda \langle n|V|n\rangle + \lambda^2 \sum_{k\neq n} \frac{|\langle k|V|n\rangle|^2}{E_n^{(0)} - E_k^{(0)}}$$

$$+\lambda^3 \left(-\langle n|V|n\rangle \sum_{k\neq n} \frac{|\langle k|V|n\rangle|^2}{(E_n^{(0)} - E_k^{(0)})^2} + \sum_{k\neq n}\sum_{m\neq n} \frac{\langle n|V|m\rangle \langle m|V|k\rangle \langle k|V|n\rangle}{(E_n^{(0)} - E_k^{(0)})(E_n^{(0)} - E_m^{(0)})} \right) + \cdots$$

At each order in the expansion, we find pole structures when energy levels are very close.

⟶ Numerically, this approximation is not good when the energy gap is $\mathcal{O}(\lambda)$ [resummation is needed]

Two-level system example

If the first excited state is close to the ground state, while all other states are far-separated,

⟶ the leading approximation for lowest two states is a two-level system

Example: $H = \frac{B}{2}\sigma_z + \lambda(3\sigma_x + \sigma_z)$

$|B|$ is the energy gap for "free" Hamiltonian $H_0 = \frac{B}{2}\sigma_z$

Perturbative expansion for the ground state energy

$$E_g = -\frac{B}{2} - \lambda - \frac{9\lambda^2}{B} + \frac{18\lambda^3}{B^2} + \frac{45\lambda^4}{B^3} - \frac{414\lambda^5}{B^4} + \cdots \qquad B > 0$$

Not easy to resum if one does not recognize the pattern of coefficients

Hellmann-Feynman theorem $\frac{dE_g}{d\lambda} = \langle\psi_g|\frac{dH}{d\lambda}|\psi_g\rangle = \frac{a_1\lambda + a_2}{\sqrt{\lambda^2 + b_1\lambda + b_2}}$ **solution** ⟶ $E_g = -\frac{1}{2}\sqrt{B^2 + 4B\lambda + 40\lambda^2}$

But everyone knows there is a straightforward way! [direct diagonalization]

$$\det(H - EI) = E^2 - (B^2/4 + B\lambda + 10\lambda^2) \longrightarrow E = \pm\frac{1}{2}\sqrt{B^2 + 4B\lambda + 40\lambda^2}$$

Avoided Level Crossing

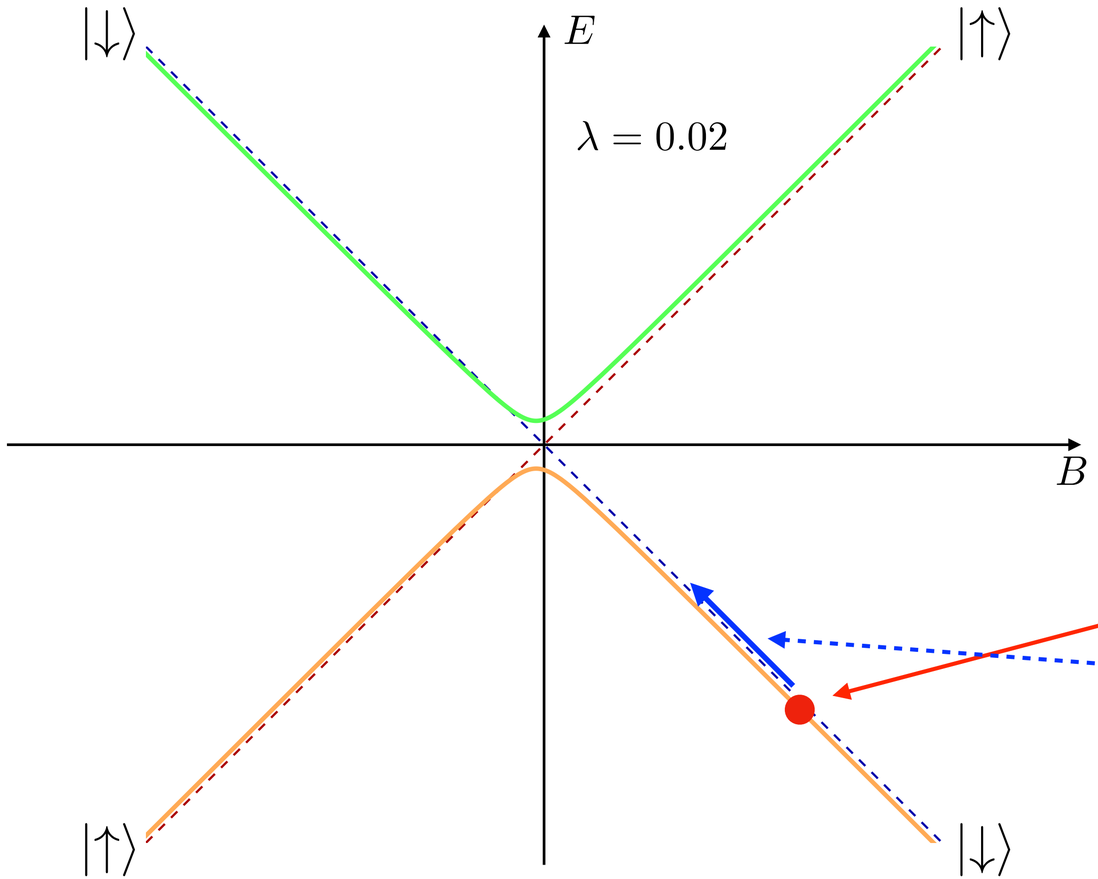

Varying the external field B, we find avoided level crossing near $B \sim 0$.

The "free" Hamiltonian has degeneracy at $B = 0$, but is lifted by small perturbation.

Comparison btw two methods:

1. Perturbation + resummation

   [may not know the existence of the second level]

   Apply perturbation within the valid regime

   Resum the series near the intersection

2. The existence of the second level is known, the direct diagonalization is much simpler.

Avoided Level Crossing

Avoided level crossing is a general phenomenon in physics.

The immediate impact of avoided level crossing in a degenerate two state system is the emergence of a lowered energy eigenstate.

https://en.wikipedia.org/wiki/Avoided_crossing

Quantum Resonance: e.g. benzene

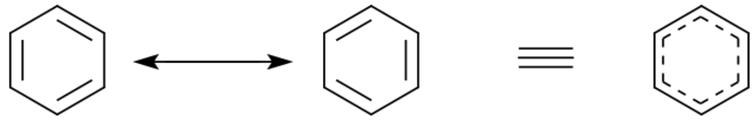

have the same e.v. $\langle H \rangle$

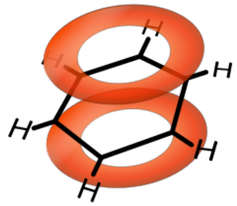

delocalized pi system

In solid physics, the avoided crossing can have an influence on the band structures.

Nearly free electron model: single electron spectrum

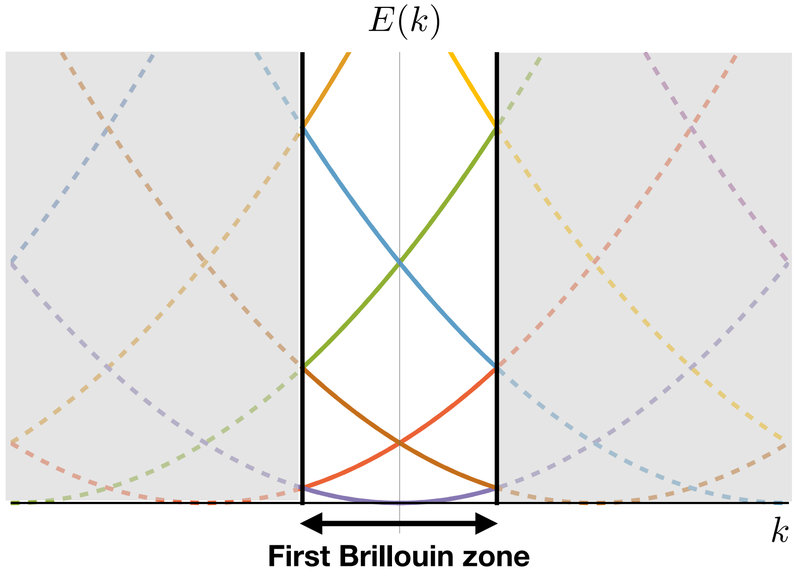

Turn on lattice potential

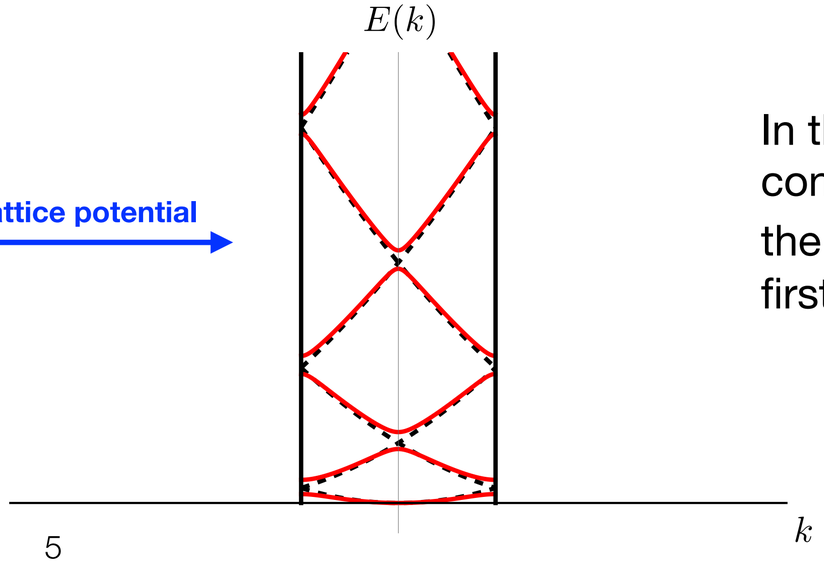

In this example, the continuous parameter is the momentum k in the first Brillouin zone.

Avoided Level Crossing in Gauge Theories

Gauge/String Duality

[Brower, Polchinski, Strassler, Tan, 2006]

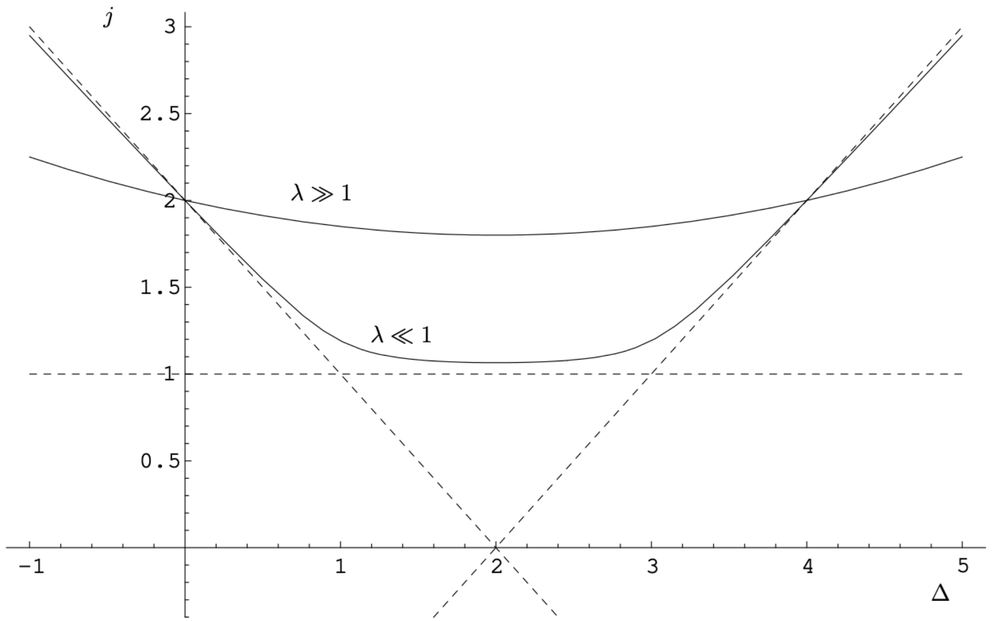

Integrability of planar $\mathcal{N} = 4$ SYM

[Gromov, Levkovich-Maslyuk, Sizov, 2015]

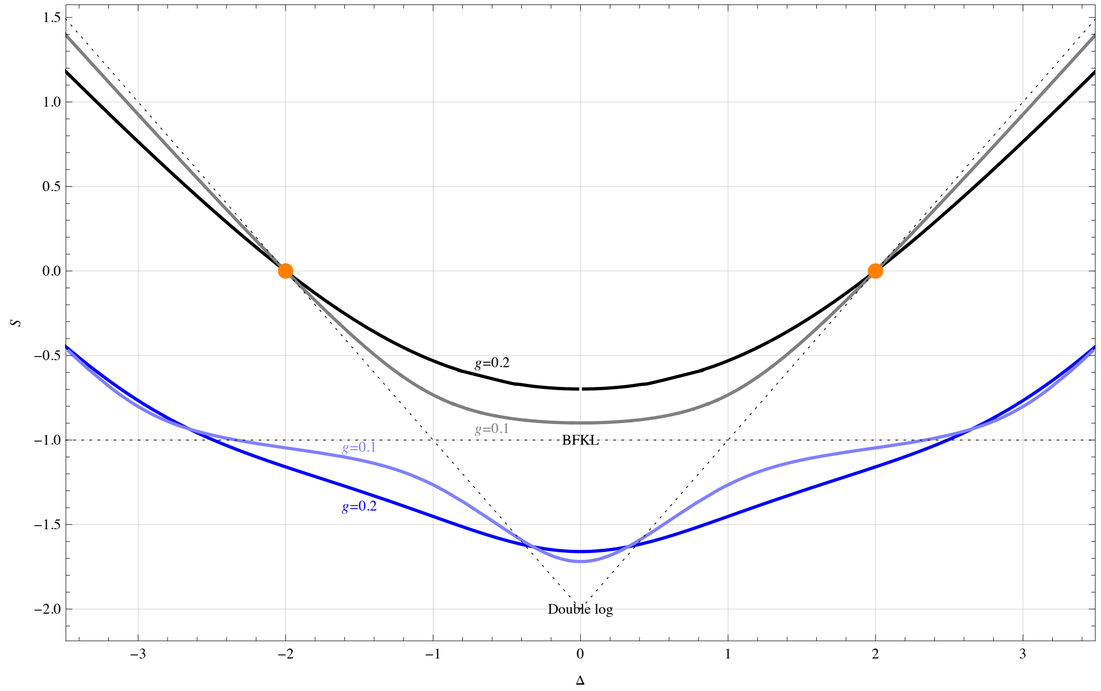

Avoided Level Crossing in Gauge Theories

Gauge/String Duality

[Brower, Polchinski, Strassler, Tan, 2006]

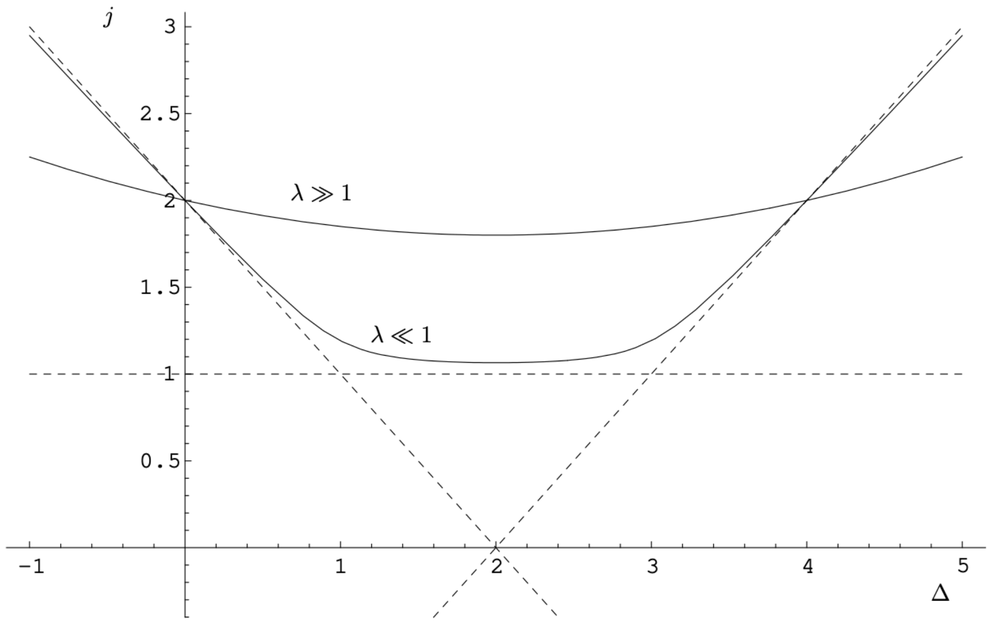

Integrability of planar $\mathcal{N} = 4$ SYM

[Gromov, Levkovich-Maslyuk, Sizov, 2015]

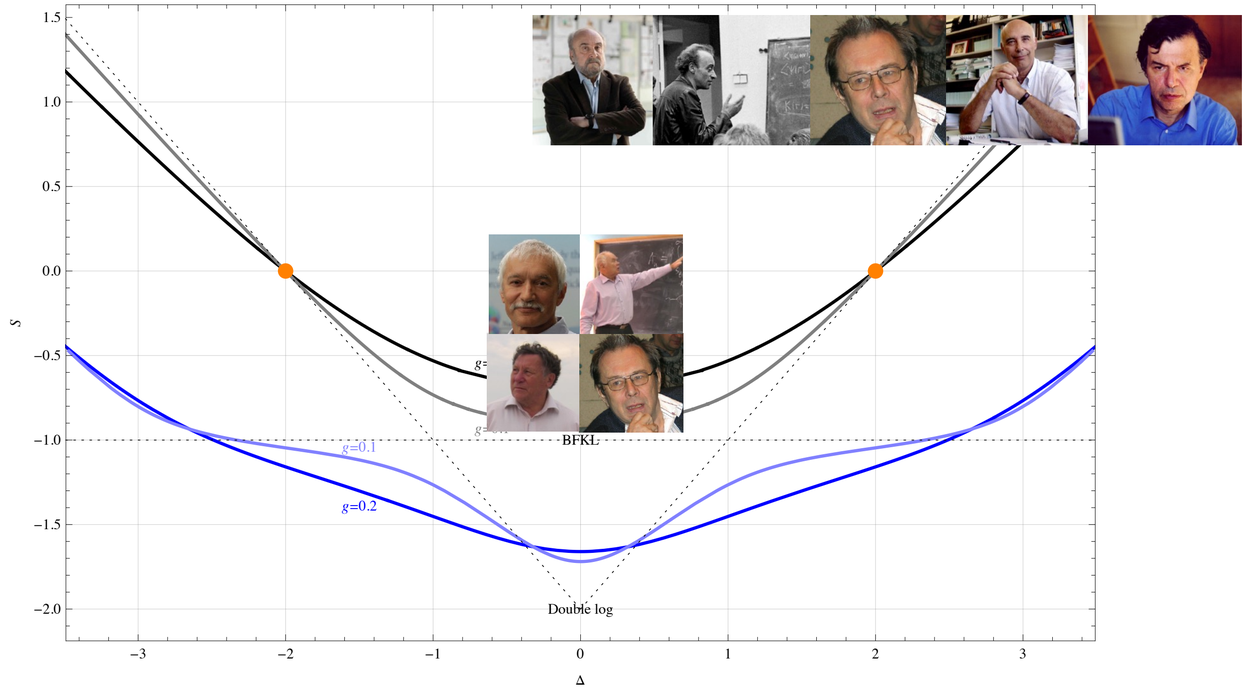

Avoided Crossing in QCD

pure gluon Chew-Frautschi Plot → add quarks → QCD Chew-Frautschi Plot

local operator spin/detector dimension*

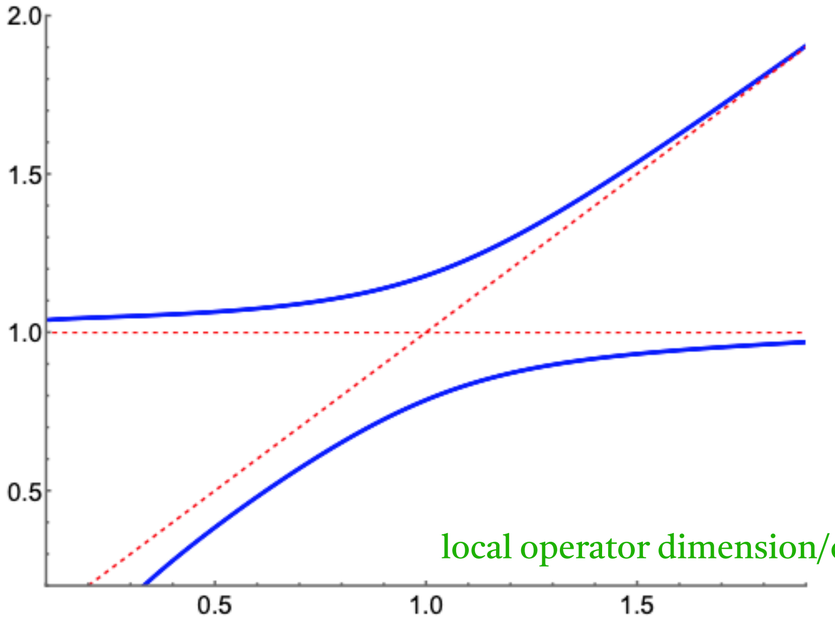

local operator dimension/detector spin*

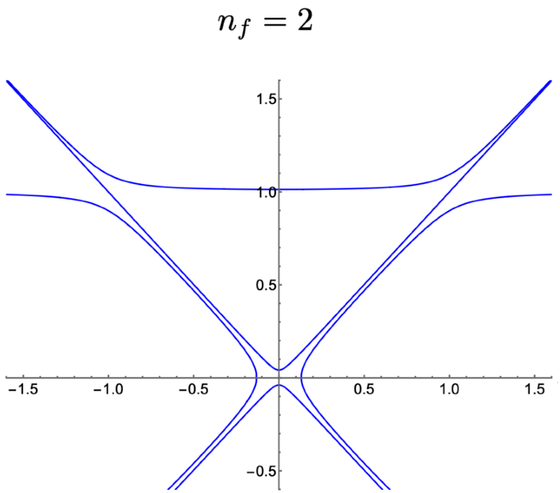

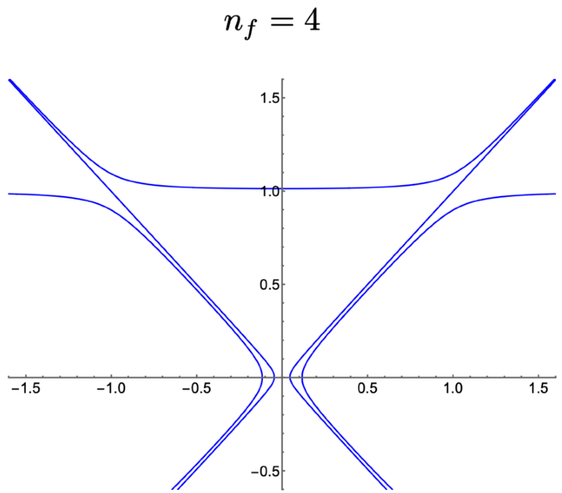

* there may be a possible constant shift and a minus sign.

See Cyuan-Han's Talk

Light-ray Operators

- The most important example of light-ray operator is energy flow operator/calorimeter/ANEC operator.

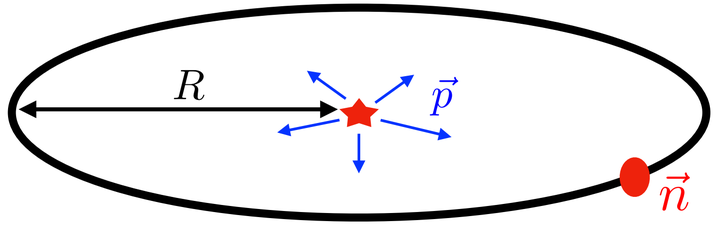

- The energy flow operator is a non-local operator defined on a light-ray located at future null infinity

$$\mathcal{E}(\vec{n}) = \lim_{r\to\infty} r^2 \int_0^\infty dt\, \vec{n}_i T^{0i}(t, r\vec{n})$$

[Sveshnikov, Tkachov, 1996; Hofman, Maldacena, 2008;…]

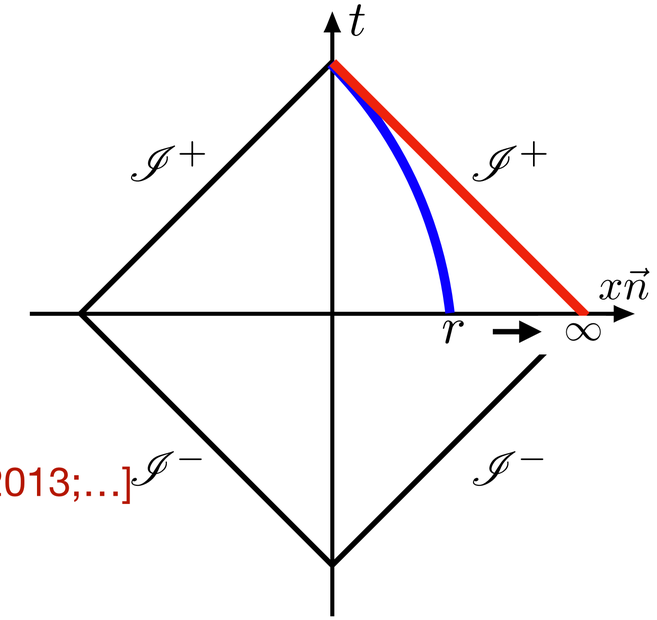

- Relation to collider observables

[Hofman, Maldacena, 2008; Belitsky, Hohenegger, Korchemsky, Sokatchev, Zhiboedov, 2013;…]

- Generalization to other local operators

$$\mathbf{L}[\mathcal{O}](x, n) = \int_{-\infty}^{\infty} d\alpha (-\alpha)^{-\Delta-J} \mathcal{O}\left(x - \frac{n}{\alpha}, n\right)$$

direction

starting point

[Kravchuk, Simmons-Duffin, 2018]

Examples of more general light-ray operators, see [Chang, Kologlu, Kravchuk, Simmons-Duffin, Zhiboedov, 2020; Caron-Huot, Kologlu, Kravchuk, Meltzer, Simmons-Duffin, 2022;…]

Interesting Objects for studying Lorentzian Dynamics

DGLAP Operators in QCD

For unpolarized cases, there are only two kinds of twist-2 operators in QCD

Local Operators

$$\mathcal{O}_q^{[J]} = \frac{1}{2^J}\bar{\psi}\gamma^+(iD^+)^{J-1}\psi$$

$$\mathcal{O}_g^{[J]} = -\frac{1}{2^J}F_a^{\mu+}(iD^+)^{J-2}F_a^{\mu+}$$

$$\lim_{r\to\infty} r^2 \int_0^\infty dt$$

Light Transform

Light-ray Operators

$$\mathbb{O}_q^{[J]}(\vec{n}) = \mathcal{D}^q_{J_L}(n)$$

$$\mathbb{O}_g^{[J]}(\vec{n}) = \mathcal{D}^g_{J_L}(n)$$

J_L is the spin of light-ray operator, which is more useful than label J in the mixing problem. For bare DGLAP detectors, $J_L = -1-J$.

The analytic continuation of even spin branch is

Physics Interpretation
[in free theory]
Measuring E^{J-1}

$$\mathbb{O}_q^{[J]}(\vec{n}) = \sum_s \int \frac{d^3p}{(2\pi)^3 2E}\delta^{(2)}(\hat{p}-\vec{n})\, E^{J-1}(b^\dagger_{\vec{p},s}b_{\vec{p},s} + d^\dagger_{\vec{p},s}d_{\vec{p},s})$$

$$\mathbb{O}_g^{[J]}(\vec{n}) = \sum_{\lambda,c} \int \frac{d^3p}{(2\pi)^3 2E}\delta^{(2)}(\hat{p}-\vec{n})\, E^{J-1}\, a^\dagger_{\vec{p},\lambda,c}a_{\vec{p},\lambda,c}$$

Not IR-safe measurement

[HC, Moult, Zhu, 2021]

Analyticity in Spin

[S-matrix: Gribov-Froissart formula;
CFT: Caron-Huot, 2017]

Physical interpretation of continuous operator spectrum:

Light-ray operators are expected to be the **analytic continuation** of local operators.

[Kravchuk, Simmons-Duffin, 2018]

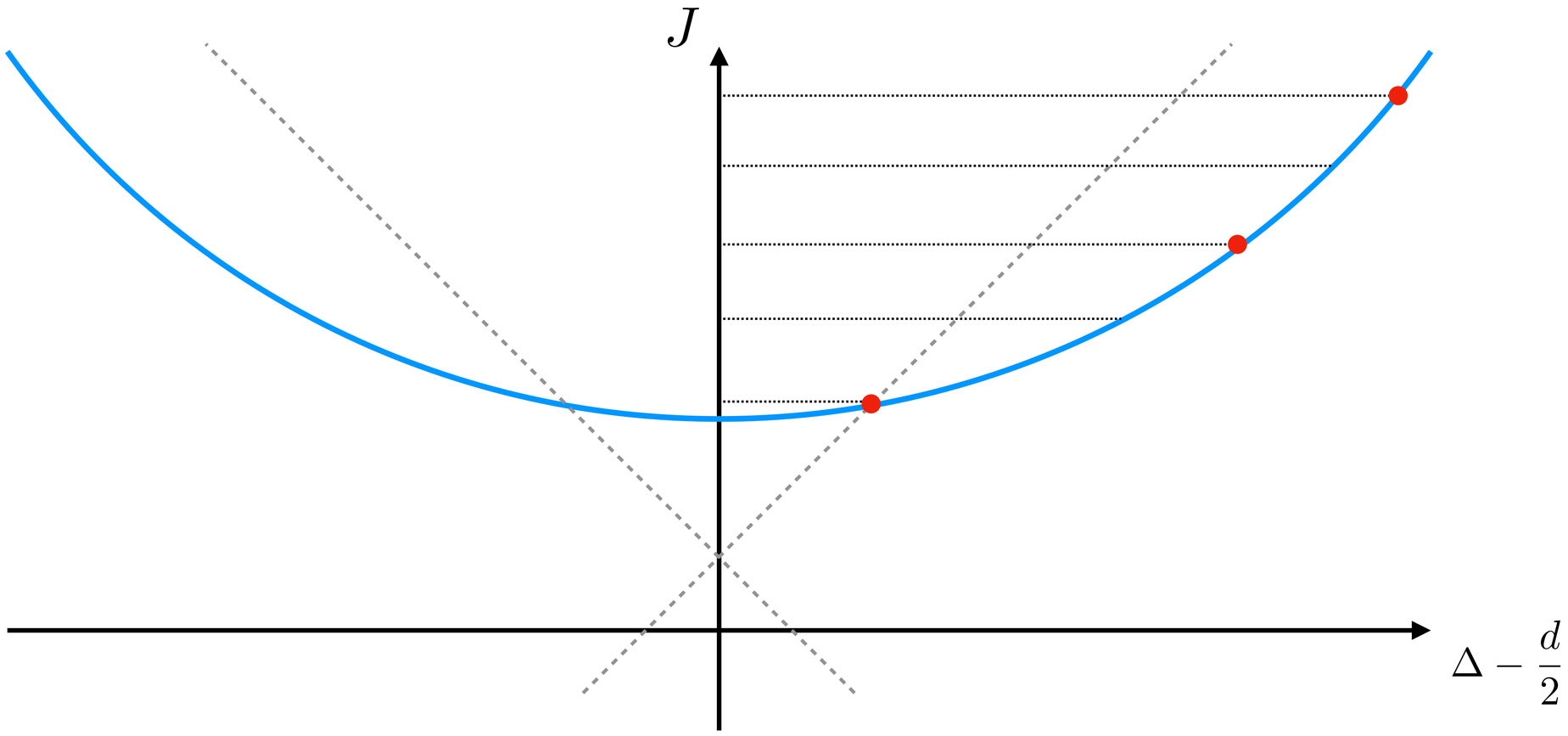

Structures of DGLAP/BFKL mixing

BFKL detector

$$\mathcal{D}^{\mathrm{BFKL}}_{J_L}(z) = \frac{\Gamma(J_L+d-2)}{\Gamma(\frac{J_L+d-2}{2})^2}\int d^{d-2}z_i d^{d-2}z_j \left(\frac{2z_i\cdot z_j}{(2z\cdot z_i)(2z\cdot z_j)}\right)^{-J_L/2}\mathcal{N}^c(z_i)\mathcal{N}^c(z_j)$$

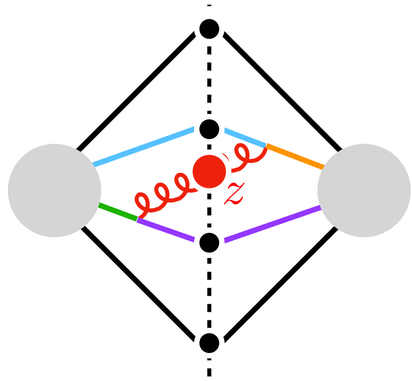

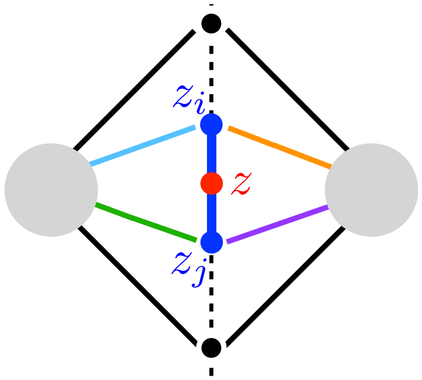

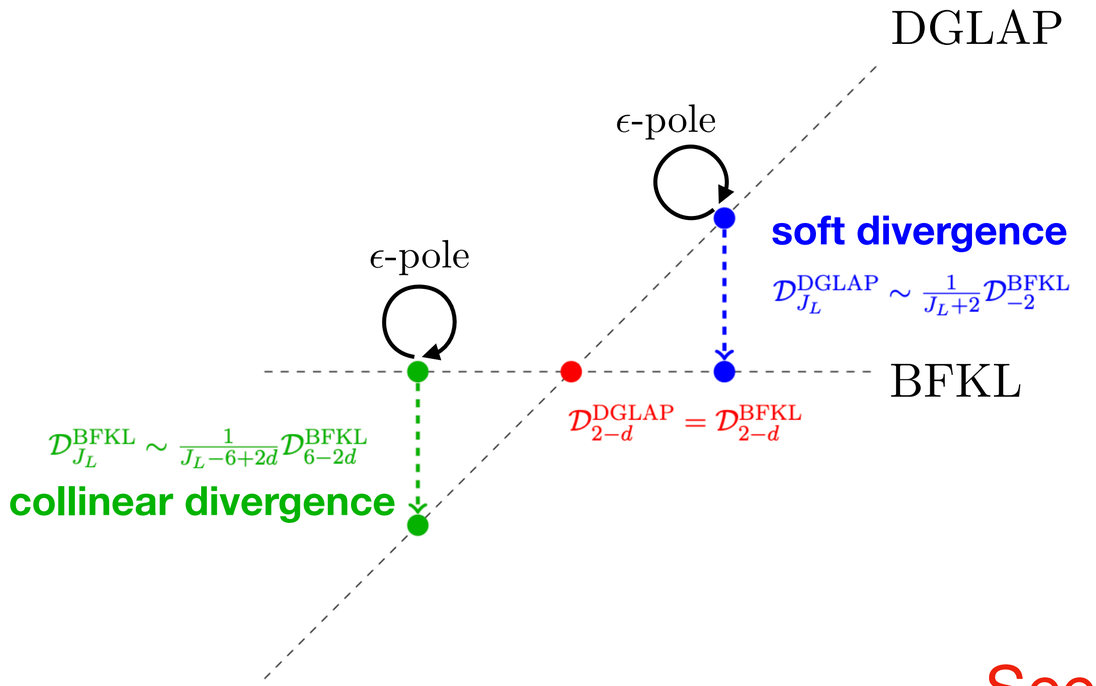

See Cyuan-Han's Talk

The mixing story may sound nice theoretically…

but in a practical sense,

the BFKL detector is not measurable in a real-world experiment!

- final states are hadrons, impossible to impose color interference

Why should one care about this weird detector?

The mixing story may sound nice theoretically…

but in a practical sense,

the BFKL detector is not measurable in a real-world experiment!

Why should one care about this weird detector?

Philosophy: These perturbative detectors show up as intermediate states.

Simplest Family of Observables in Experiments

One-point event shapes/DGLAP-type “hadron” detectors*

*Here “hadron” is to emphasize all particles after hadronization.

In the high-energy scattering, we assume the hadrons are almost massless.

The simplest detectors do not distinguish the particle species

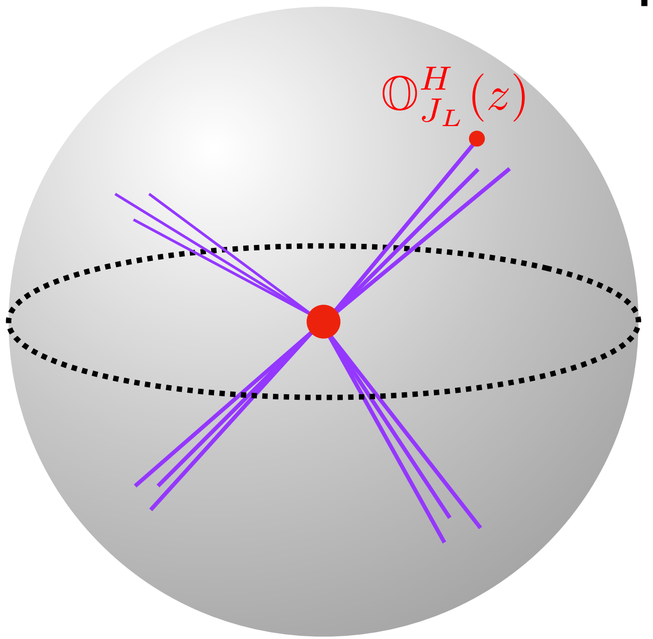

$$\mathbb{O}^H_{J_L}(z) = \sum_h \int \frac{d^3\vec{p}}{(2\pi)^3 2E} \delta^{(2)}(\hat{p} - \hat{z})\, E^{\nu-1} a_h^\dagger(p) a_h(p)$$

$\nu = -1 - J_L$

sum over all particles

For example, we can measure the observables in the e^+e^- collider

$$f(\nu, Q) = \frac{1}{\sigma_{\text{tot}}} \sum_X \int d\sigma_{e^+e^-\to X} \boxed{\sum_{h\in X} \left(\frac{E_a}{Q}\right)^{\nu-1}} = \frac{4\pi}{\sigma_{\text{tot}}} \frac{\langle \mathbb{O}^H_{J_L}(z) \rangle_Q}{Q^{\nu-1}}$$

measurement function

c.o.m. energy

$\nu = 2$: energy

$\nu = 1$: multiplicity

These are not IR-safe observables! (except $\nu = 2$)

Simplest Family of Observables in Experiments

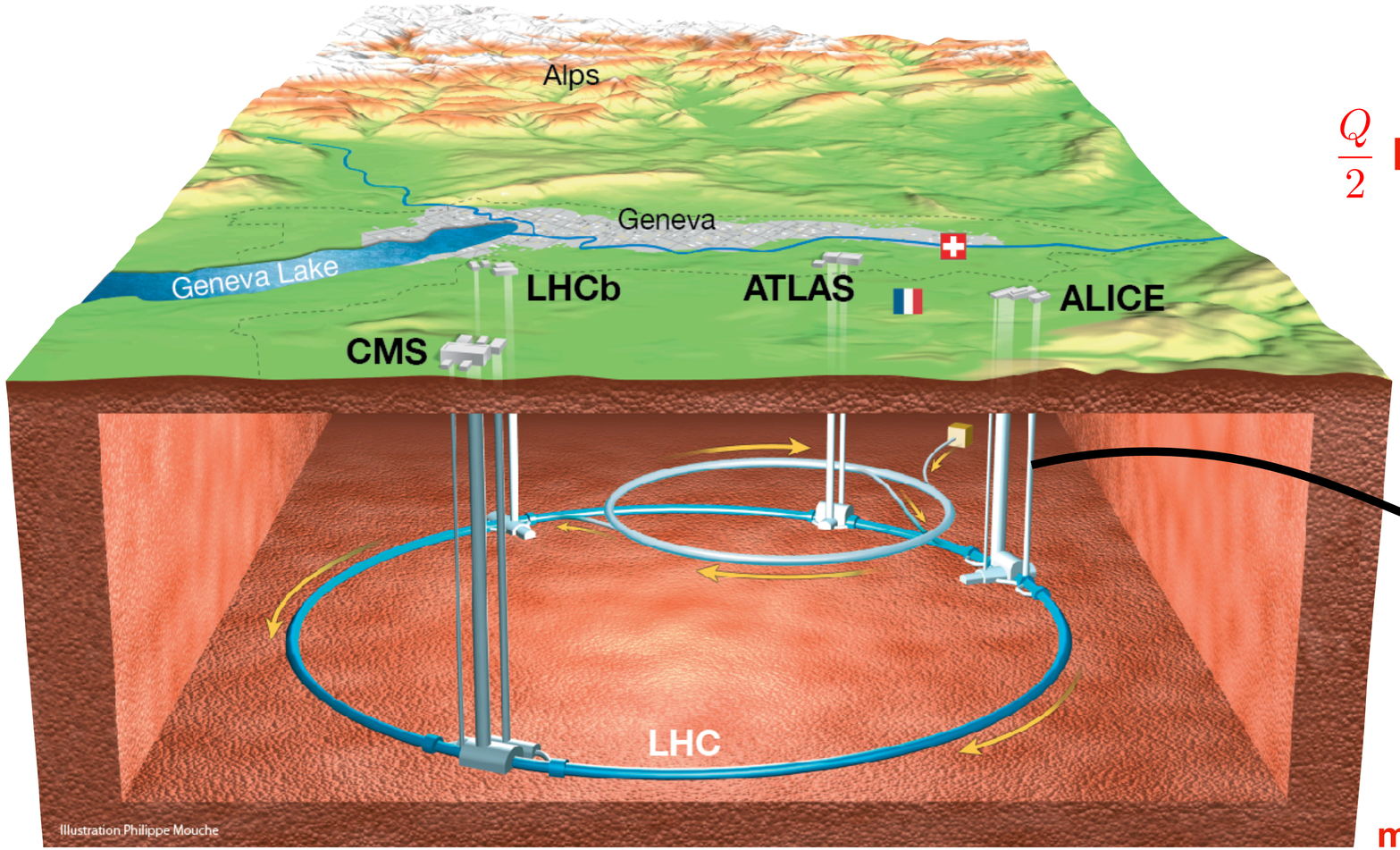

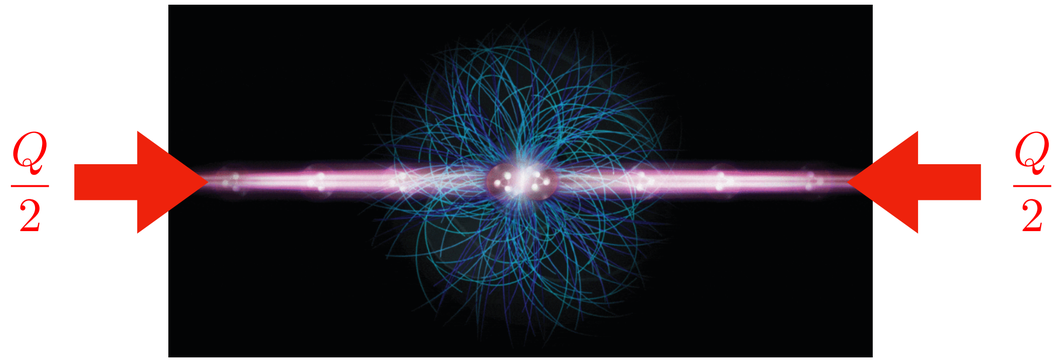

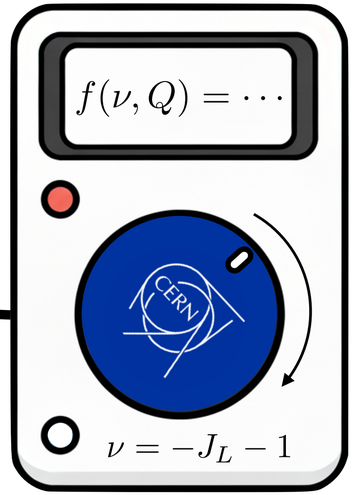

measurement function

$$f(\nu,Q) = \frac{1}{\sigma_{\text{tot}}} \sum_X \int d\sigma_{e^+e^- \to X} \boxed{\sum_{h \in X} \left(\frac{E_a}{Q}\right)^{\nu-1}} = \frac{4\pi}{\sigma_{\text{tot}}} \frac{\langle \mathbb{O}^H_{J_L}(z) \rangle_Q}{Q^{\nu-1}}$$

Factorization Picture in QCD

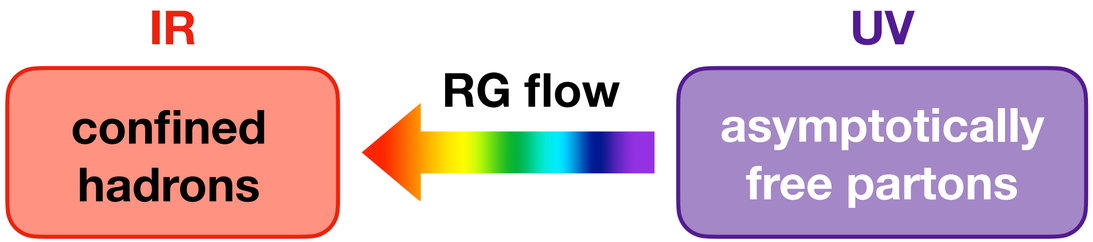

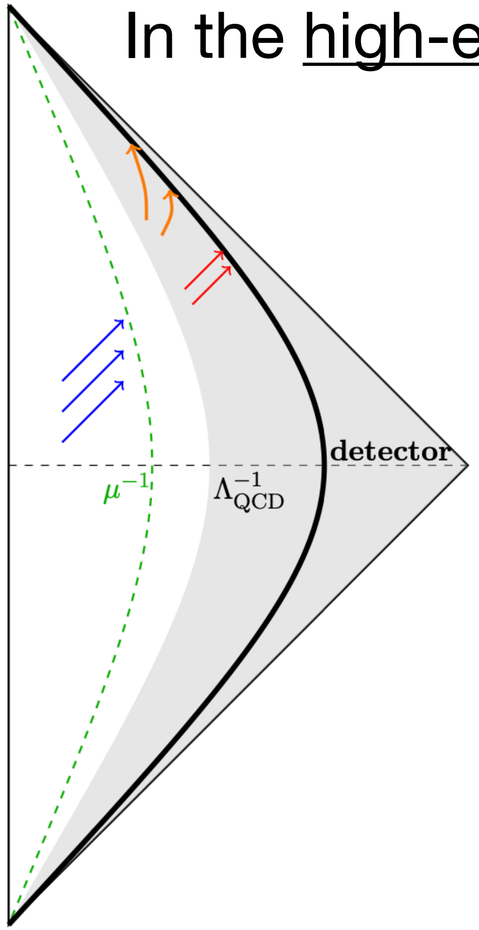

In the high-energy limit, we can **factorize** QCD observables into

perturbative part and non-perturbative part.

[asymptotic freedom] [confinement]

We can find a factorization scale μ s.t. $Q \gg \mu \gg \Lambda_{\rm QCD}$

For hard scattering length scale $\frac{1}{Q}$, $\frac{1}{\mu}$ can be approximated as pert. infinity.

In our case, the factorization is

the matching of hadronic detectors onto parton detectors.

$$\mathbb{O}^H_{J_L}(z) \sim \sum_k C_k(J_L,\mu)\,\mathcal{D}^{\rm ren}_{J_L,k}(z;\mu)$$

Wilson coefficients that contain hadronization information

Comparison with Local Operators

Example: $\mathcal{L}_{\rm BSM}[\mathcal{O}_i^{\rm UV}, \Lambda_{\rm BSM}] \sim \mathcal{L}_{\rm SM} + \sum_k \frac{a_k}{\Lambda_{\rm BSM}^{\Delta_k - d}} \mathcal{O}_k^{\rm IR}$

composite operators with Standard Model fields

from a UV BSM operator to IR SM operators

local operator matching: $\langle \Psi_{\rm IR} | \mathcal{O}_i^{\rm UV}(0) | \Psi_{\rm IR} \rangle \sim \sum_k C_k \langle \Psi_{\rm IR} | \mathcal{O}_k^{\rm IR}(0) | \Psi_{\rm IR} \rangle$

Comparison with Local Operators

Example: $\mathcal{L}_{\rm BSM}[\mathcal{O}_i^{\rm UV}, \Lambda_{\rm BSM}] \sim \mathcal{L}_{\rm SM} + \sum_k \frac{a_k}{\Lambda_{\rm BSM}^{\Delta_k - d}} \mathcal{O}_k^{\rm IR}$

composite operators with Standard Model fields

from a UV BSM operator to IR SM operators

local operator matching: $\langle \Psi_{\rm IR} | \mathcal{O}_i^{\rm UV}(0) | \Psi_{\rm IR} \rangle \sim \sum_k C_k \langle \Psi_{\rm IR} | \mathcal{O}_k^{\rm IR}(0) | \Psi_{\rm IR} \rangle$

dimensional analysis $C_k \sim \Lambda_{\rm BSM}^{\Delta_i - \Delta_k}$

Comparison with Local Operators

Example: $\mathcal{L}_{\rm BSM}[\mathcal{O}_i^{\rm UV}, \Lambda_{\rm BSM}] \sim \mathcal{L}_{\rm SM} + \sum_k \frac{a_k}{\Lambda_{\rm BSM}^{\Delta_k - d}} \mathcal{O}_k^{\rm IR}$

composite operators with Standard Model fields

from a UV BSM operator to IR SM operators

local operator matching: $\langle \Psi_{\rm IR} | \mathcal{O}_i^{\rm UV}(0) | \Psi_{\rm IR} \rangle \sim \sum_k C_k \langle \Psi_{\rm IR} | \mathcal{O}_k^{\rm IR}(0) | \Psi_{\rm IR} \rangle \sim \Lambda_{\rm IR}^{\Delta_k + \cdots}$

dimensional analysis $C_k \sim \Lambda_{\rm BSM}^{\Delta_i - \Delta_k}$

Comparison with Local Operators

Example: $\mathcal{L}_{\rm BSM}[\mathcal{O}_i^{\rm UV}, \Lambda_{\rm BSM}] \sim \mathcal{L}_{\rm SM} + \sum_k \frac{a_k}{\Lambda_{\rm BSM}^{\Delta_k - d}} \mathcal{O}_k^{\rm IR}$

composite operators with Standard Model fields

from a UV BSM operator to IR SM operators

local operator matching: $\langle \Psi_{\rm IR} | \mathcal{O}_i^{\rm UV}(0) | \Psi_{\rm IR} \rangle \sim \sum_k C_k \langle \Psi_{\rm IR} | \mathcal{O}_k^{\rm IR}(0) | \Psi_{\rm IR} \rangle$

Lowest dimension operators dominate the matching

$\sim \left(\frac{\Lambda_{\rm IR}}{\Lambda_{\rm BSM}} \right)^{\Delta_k} \cdots$

Comparison with Local Operators

Example: $\mathcal{L}_{\rm BSM}[\mathcal{O}_i^{\rm UV}, \Lambda_{\rm BSM}] \sim \mathcal{L}_{\rm SM} + \sum_k \frac{a_k}{\Lambda_{\rm BSM}^{\Delta_k - d}} \mathcal{O}_k^{\rm IR}$

composite operators with Standard Model fields

from a UV BSM operator to IR SM operators

local operator matching: $\langle \Psi_{\rm IR} | \mathcal{O}_i^{\rm UV}(0) | \Psi_{\rm IR} \rangle \sim \sum_k C_k \langle \Psi_{\rm IR} | \mathcal{O}_k^{\rm IR}(0) | \Psi_{\rm IR} \rangle$

Lowest dimension operators dominate the matching

$\sim \left(\frac{\Lambda_{\rm IR}}{\Lambda_{\rm BSM}} \right)^{\Delta_k} \cdots$

QCD detector matching:

expand hadronic d.o.f. to partonic d.o.f.

$$\langle \Psi_{\rm UV} | \mathcal{D}_i^{\rm IR}(z) | \Psi_{\rm UV} \rangle \sim \sum_k C_k \langle \Psi_{\rm UV} | \mathcal{D}_i^{\rm UV}(z) | \Psi_{\rm UV} \rangle$$

see next page for dimensional analysis

Properties of Detector Matching

$$\langle \mathbb{O}^H_{J_L}(z)\rangle_Q \sim \sum_k C_k(J_L,\mu)\langle \mathcal{D}^{\rm ren}_{J_L,k}(z;\mu)\rangle_Q$$

$\boldsymbol{\Delta}_L = -\Delta_L$

Dimensional analysis	$[\nu-1]$	$[\nu-1-\boldsymbol{\Delta}_L]$ ←	$[\boldsymbol{\Delta}_L]$
		$\Lambda_{\rm QCD}$	Q **Typical energy scale**
		$\Lambda_{\rm QCD}^{\nu-1-\boldsymbol{\Delta}_L}$	$Q^{\boldsymbol{\Delta}_L}$ **Typical size**

Properties of Detector Matching

$$\langle \mathbb{O}^H_{J_L}(z)\rangle_Q \sim \sum_k C_k(J_L,\mu)\langle \mathcal{D}^{\rm ren}_{J_L,k}(z;\mu)\rangle_Q$$

$$\boldsymbol{\Delta}_L = -\Delta_L$$

Dimensional analysis	$[\nu-1]$	$[\nu-1-\boldsymbol{\Delta}_L]$ ←	$[\boldsymbol{\Delta}_L]$
	$\Lambda_{\rm QCD}$	Q	**Typical energy scale**
	$\Lambda_{\rm QCD}^{\nu-1-\boldsymbol{\Delta}_L}$	$Q^{\boldsymbol{\Delta}_L}$	**Typical size**

Largest dimension detector dominates the detector matching.

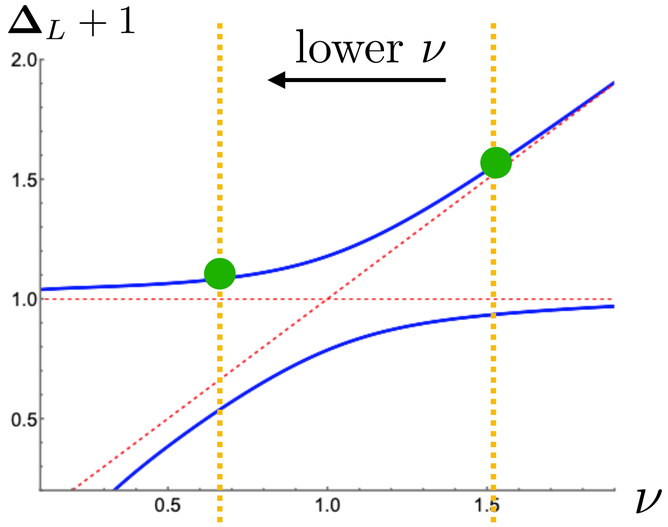

For $\nu > 1$, the dominant operator is DGLAP operators. The corresponding matching coefficients are related to the moments of the fragmentation functions.

leading approx. for
1-pt event shapes

$$f(\nu,Q) \sim Q^{\boldsymbol{\Delta}_L^{\max}-\nu+1}$$

Monte Carlo Simulation Data (Pythia)

We generate events from γ^*- and h^*-decay respectively in Pythia
at center of mass energy $Q = 250,300,350,\ldots,1000\,\mathrm{GeV}$

and fit the simulation data to the ansatz

$$f(\nu, Q) \sim Q^{\Delta_L^{\max} - \nu + 1}$$

$\nu = 0.495$

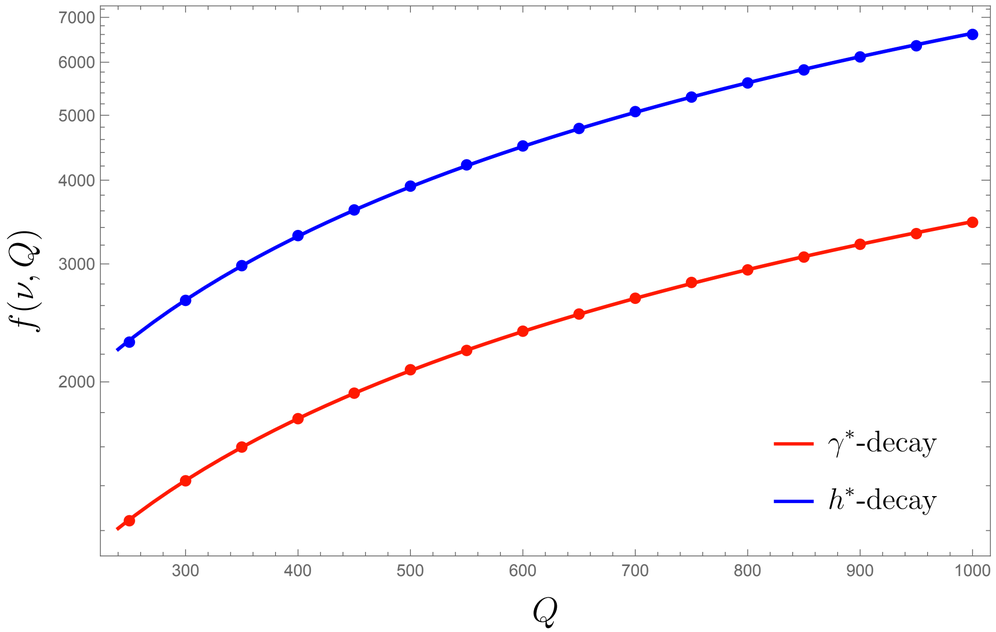

$\nu = 2.99$

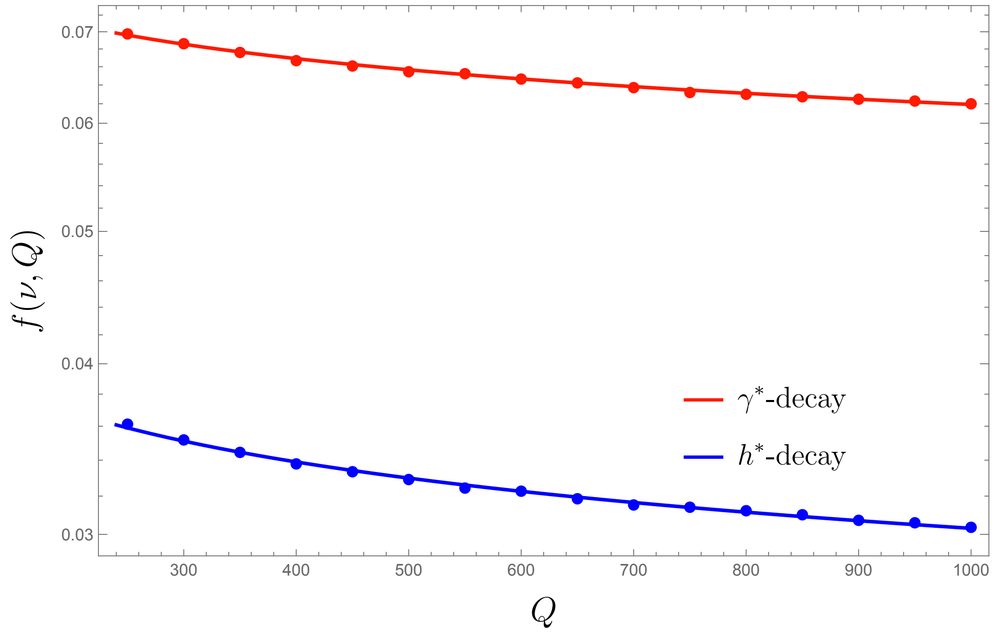

In the high energy limit, power law is a good approximation.

Monte Carlo Simulation Data (Pythia)

We generate events from γ^*- and h^*-decay respectively in Pythia
at center of mass energy $Q = 250,300,350,\ldots,1000\,\mathrm{GeV}$

and fit the simulation data to the ansatz $f(\nu, Q) \sim Q^{\Delta_L^{\max} - \nu + 1}$

Extract $\Delta_L^{\max}$

as a function of ν

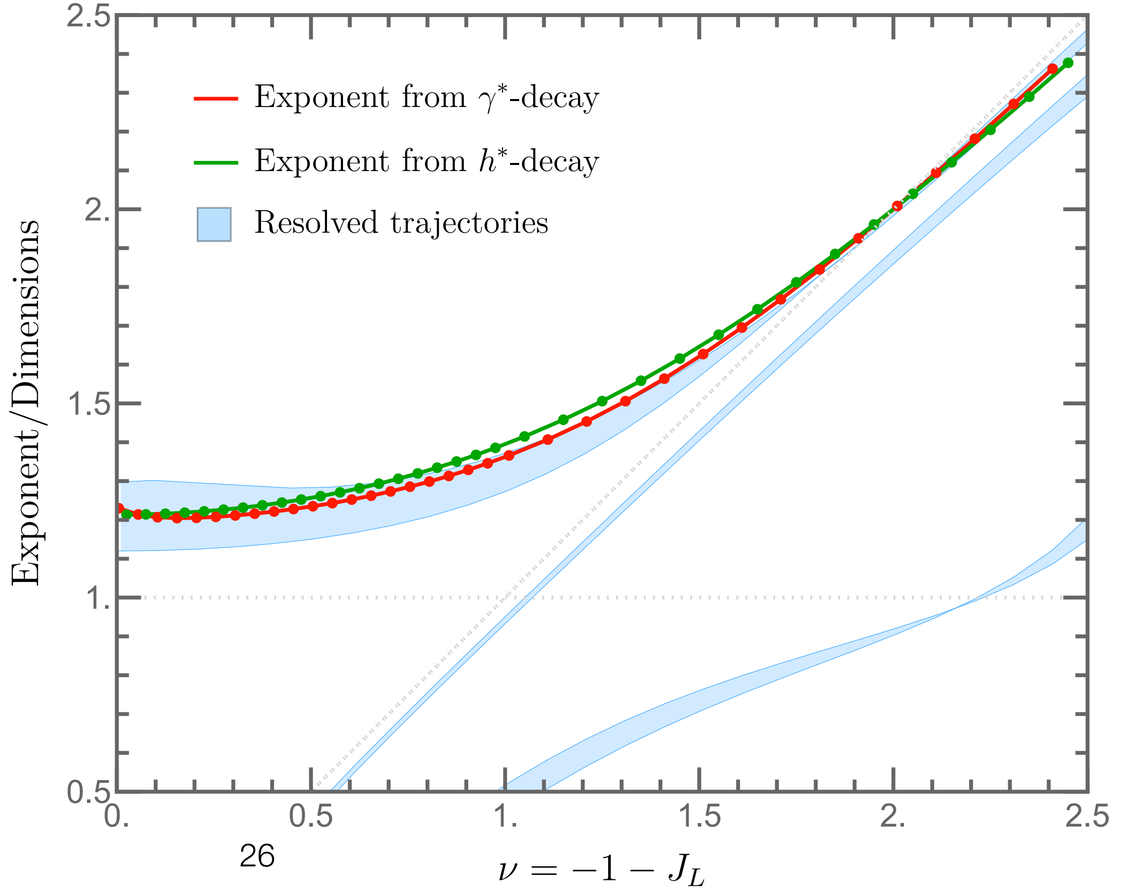

Monte Carlo Simulation Data (Pythia)

We generate events from γ^*- and h^*-decay respectively in Pythia
at center of mass energy $Q = 250,300,350,\ldots,1000\,\mathrm{GeV}$

and fit the simulation data to the ansatz $f(\nu, Q) \sim Q^{\Delta_L^{\max} - \nu + 1}$

Extract $\Delta_L^{\max}$

as a function of ν

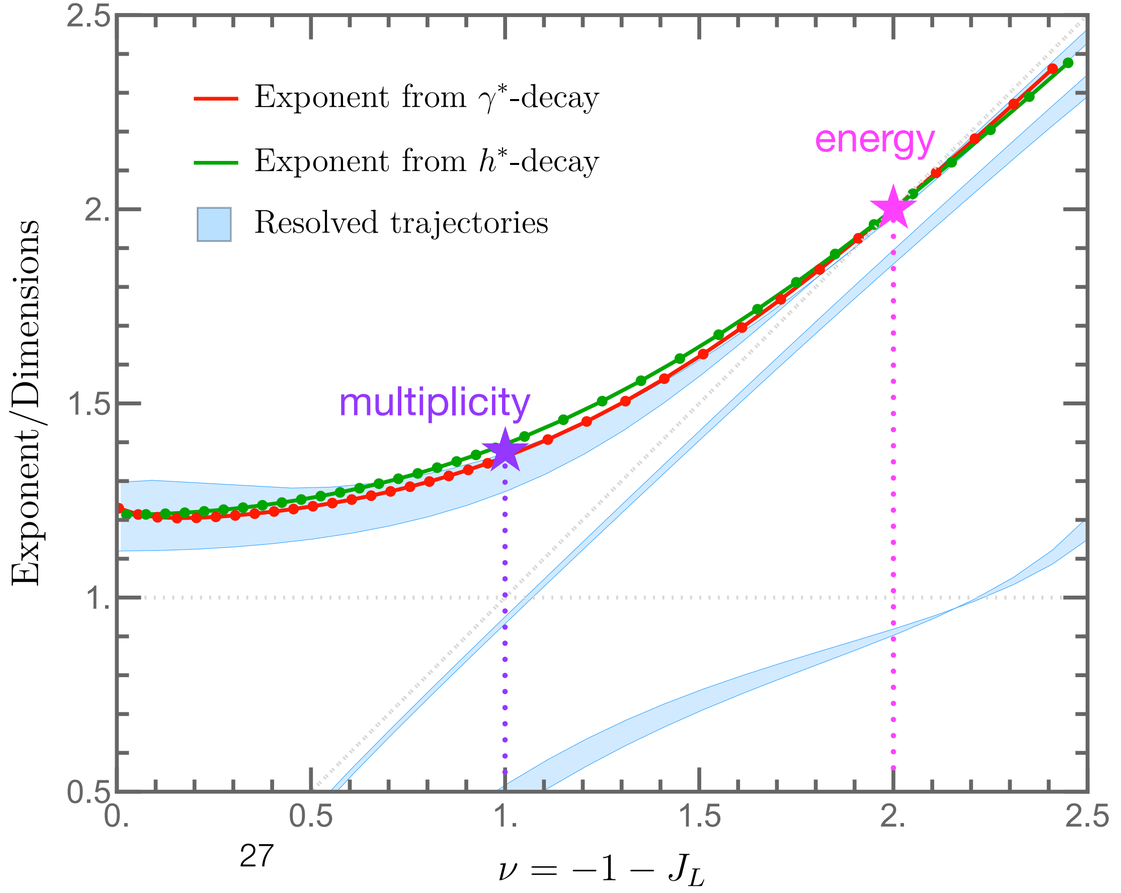

Monte Carlo Simulation Data (Pythia)

We generate events from γ^*- and h^*-decay respectively in Pythia
at center of mass energy $Q = 250,300,350,\ldots,1000\,\mathrm{GeV}$

and fit the simulation data to the ansatz $f(\nu, Q) \sim Q^{\Delta_L^{\max} - \nu + 1}$

Extract $\Delta_L^{\max}$ as a function of ν

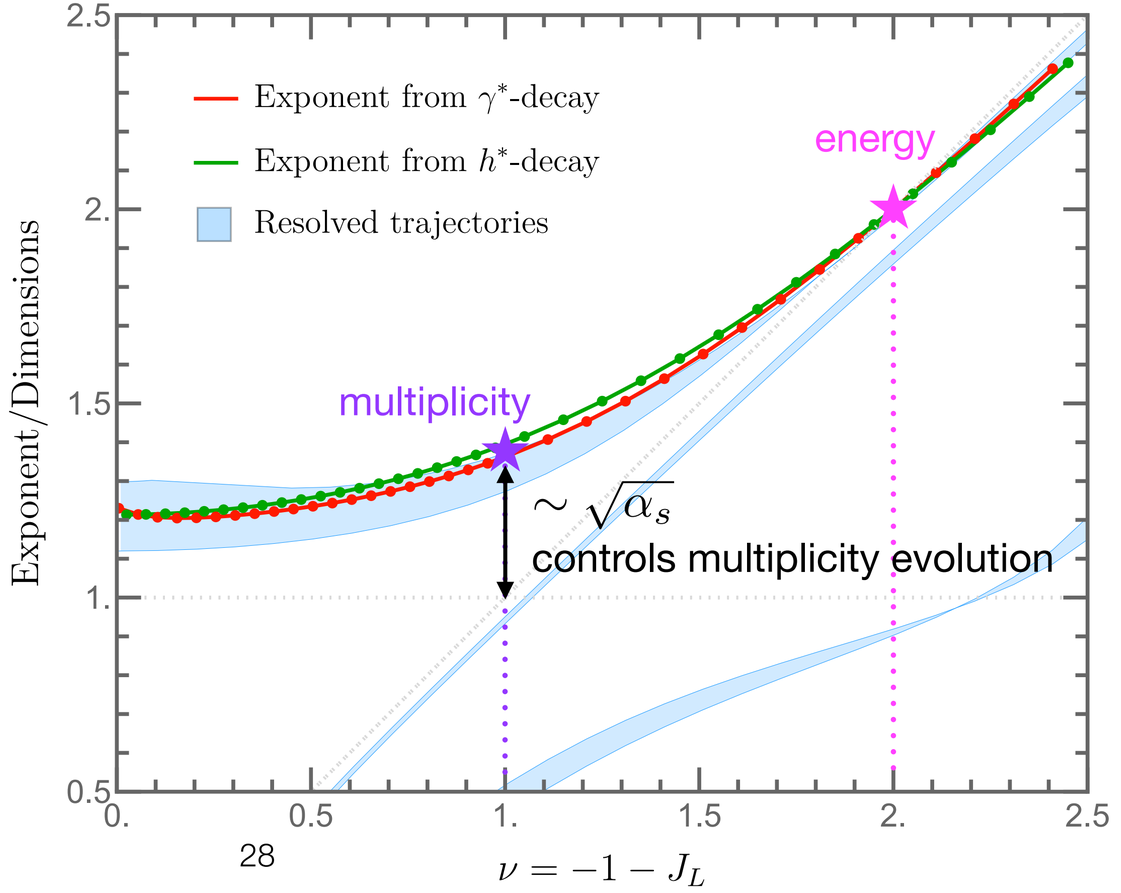

CMS Open Data

We also used the CMS Open Data with jet energy in the range [375,1125] GeV.

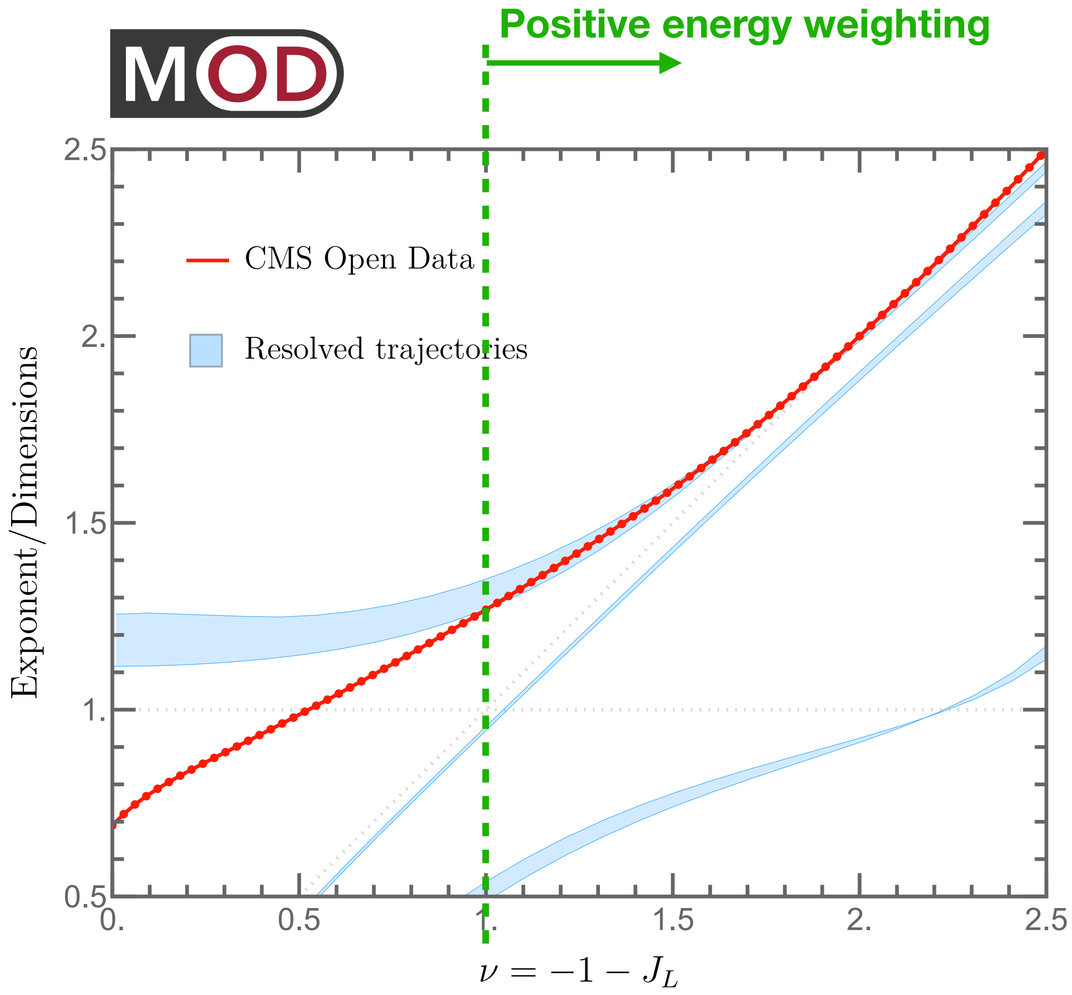

Due to the jet algorithm and other potential cuts, the negative energy weighting region might be affected.

Analytic Structure in Complex Space

When there is a level repulsion phenomenon, we can see branch cuts in complex space.

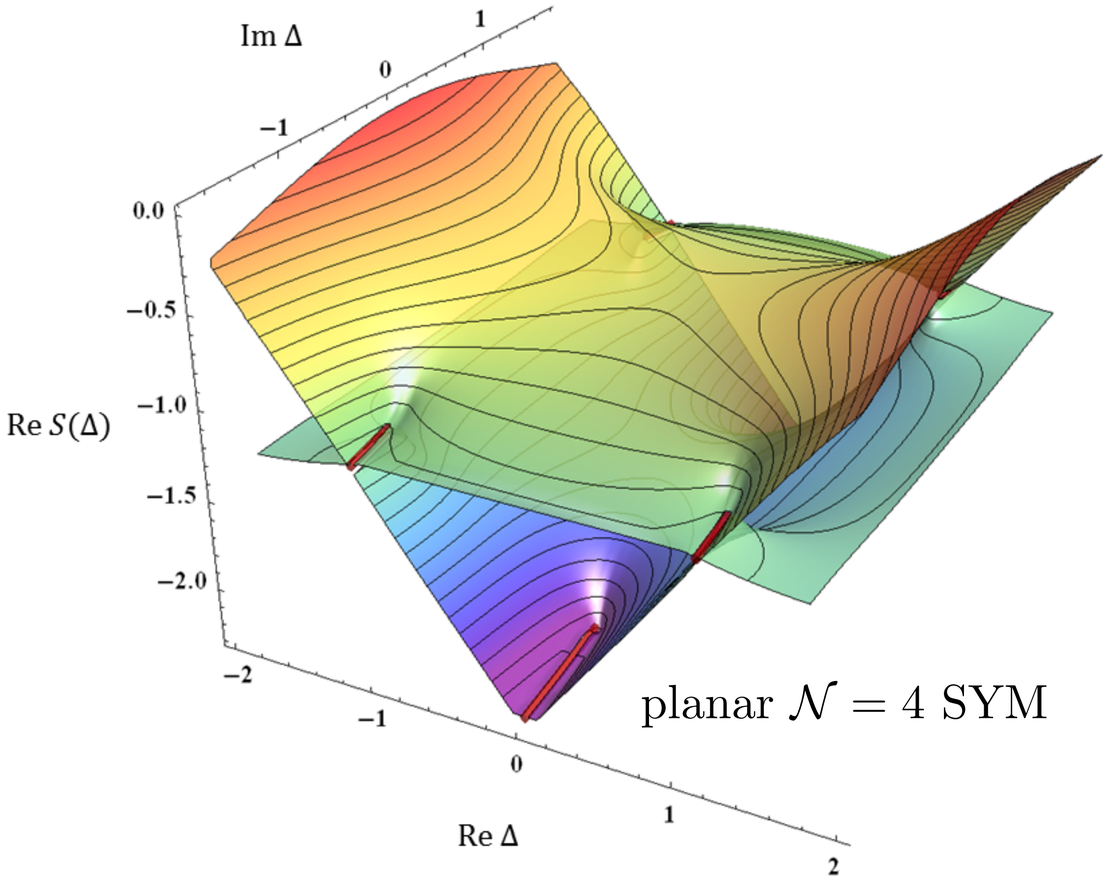

planar $\mathcal{N} = 4$ SYM

[Gromov, Levkovich-Maslyuk, Sizov, 2015]

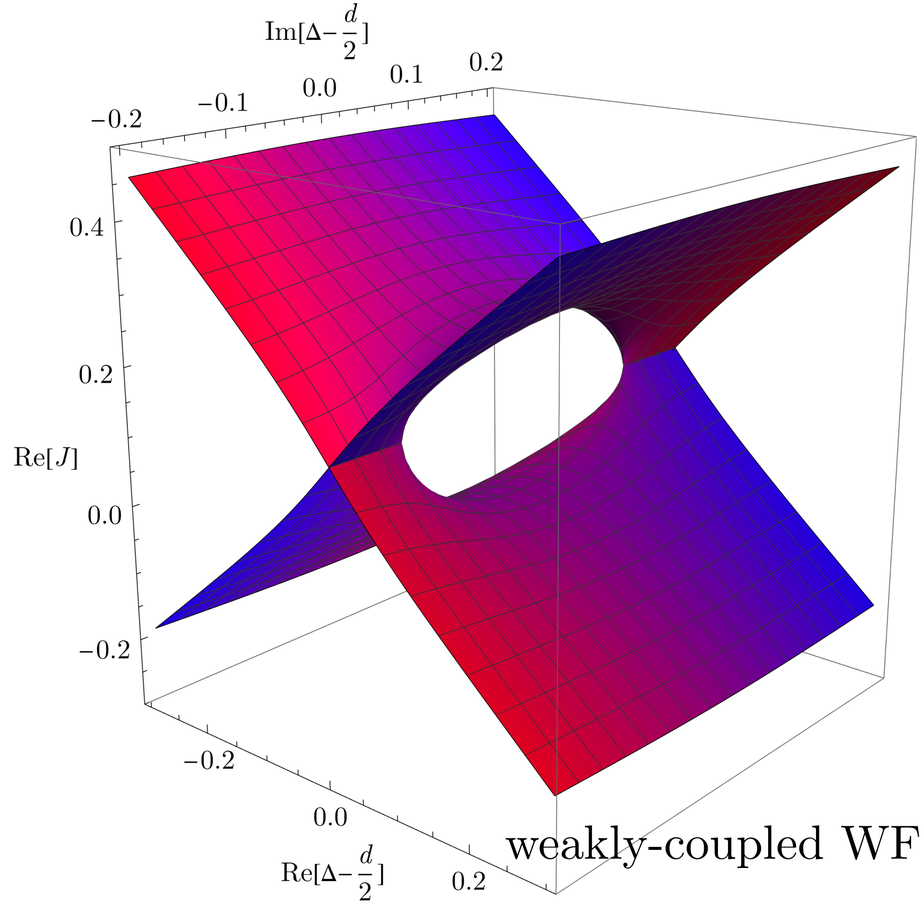

weakly-coupled WF theory

[Caron-Huot, Kologlu, Kravchuk, Meltzer, Simmons-Duffin, 2022]

Illustrative Example: Two-Level Spin System

$E = \pm\sqrt{B^2 + \lambda^2}$ Plot energy in complex space $\mathrm{Im}\, B > 0$

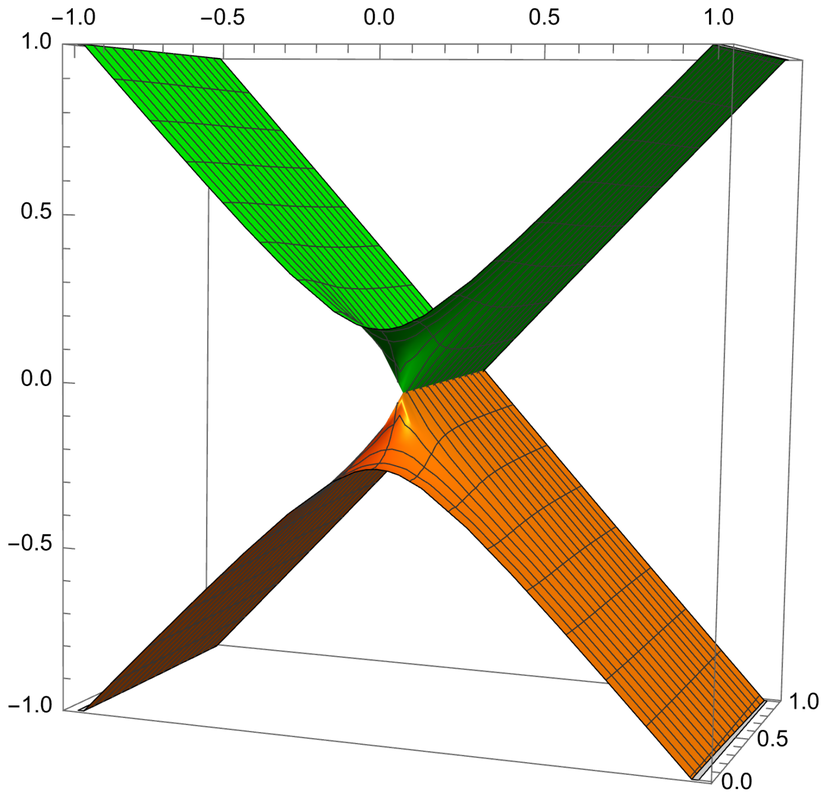

Real Part

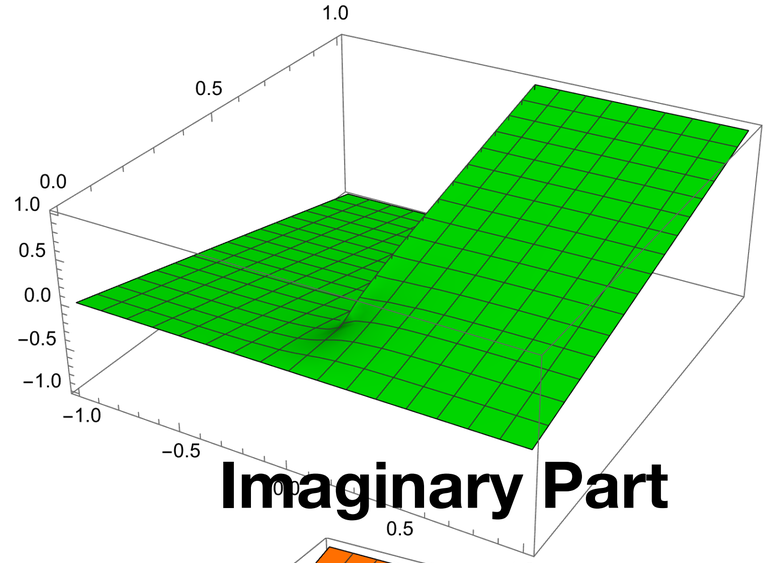

Imaginary Part

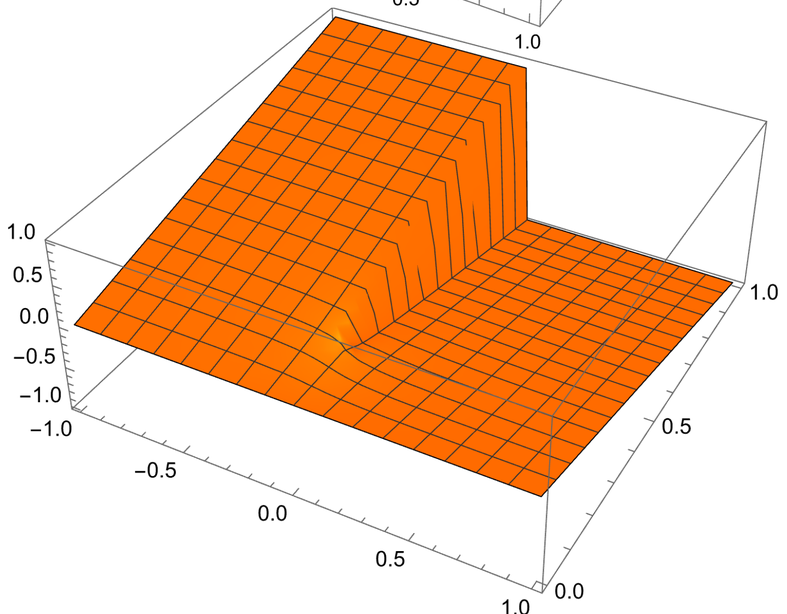

LO Top Trajectory in Complex Space

In complex space, we can easily see the branch cut from the discontinuity in the imaginary part.

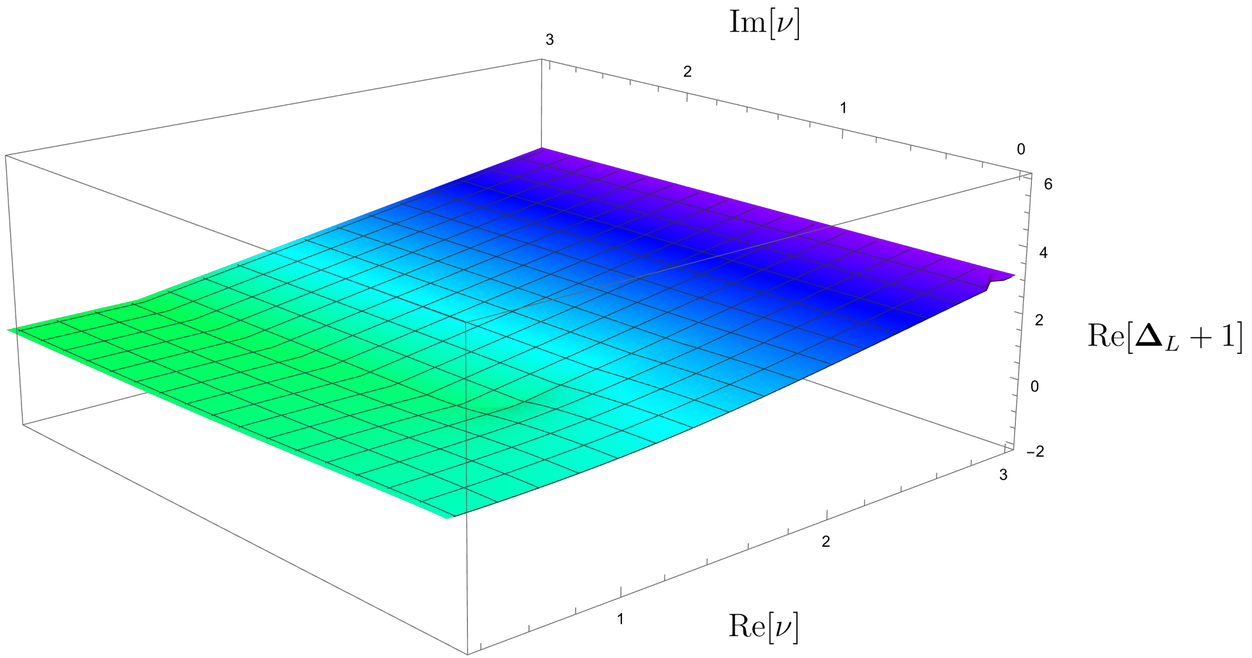

Real Part

$\alpha_s = 0.09$

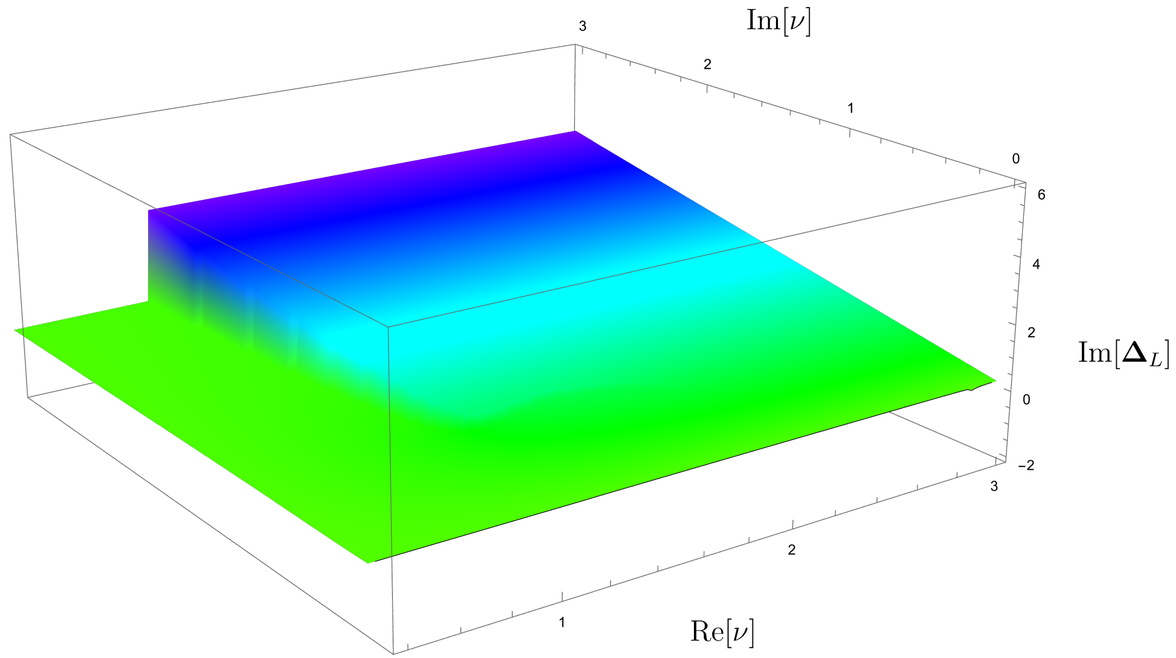

Imaginary Part

LO Top Trajectory in Complex Space

In complex space, we can easily see the branch cut from the discontinuity in the imaginary part.

Can we find similar structure in the data?

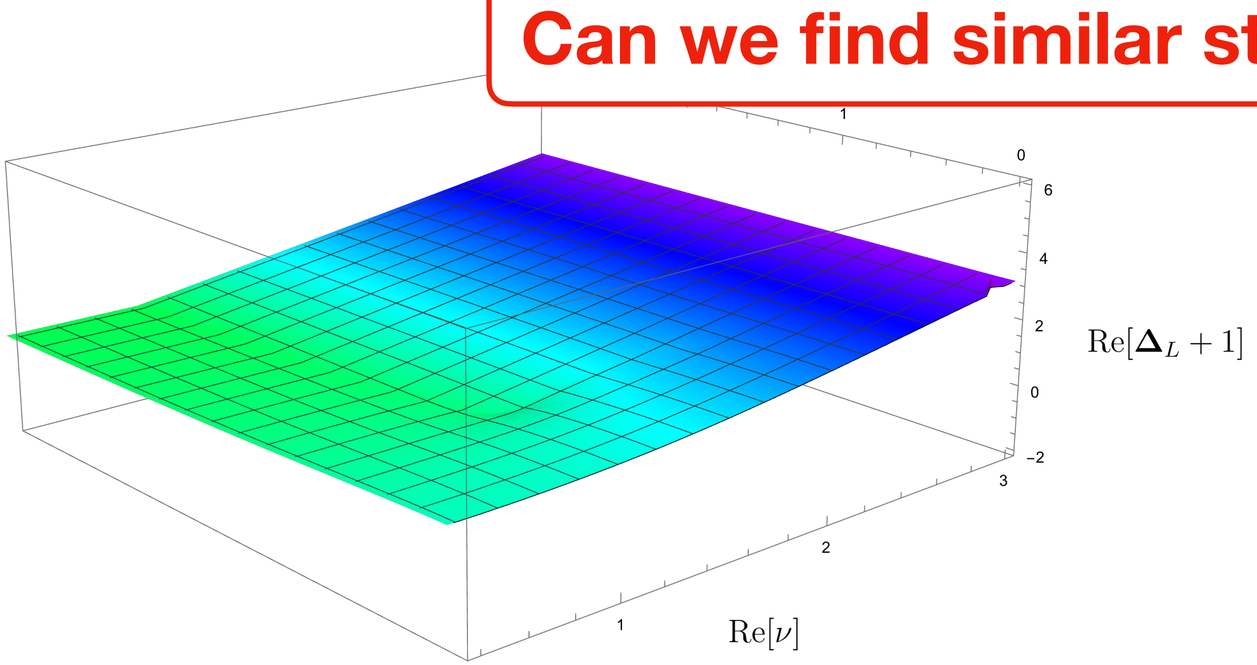

Real Part

$\alpha_s = 0.09$

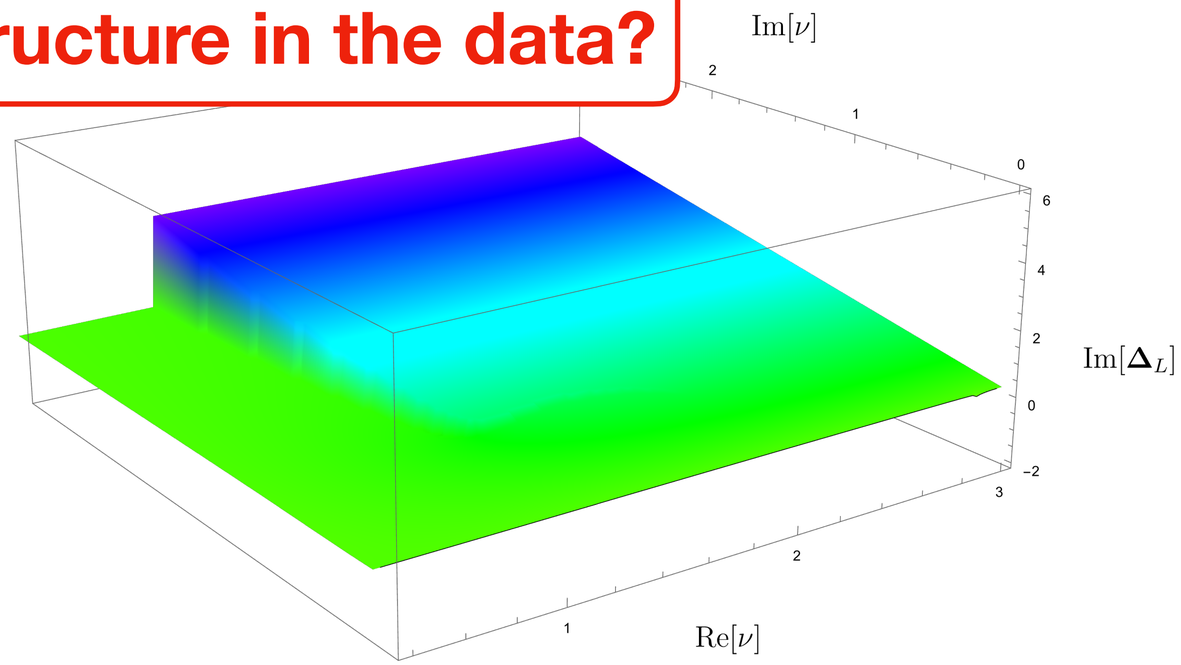

Imaginary Part

Let’s measure complexified observables!

$$f(\nu, Q) = \frac{1}{\sigma_{\text{tot}}} \sum_X \int d\sigma_{e^+e^- \to X} \sum_{h \in X} \left(\frac{E_a}{Q} \right)^{\nu-1}$$

To the best of my knowledge , this might be the first and should be the simplest non-trivial complexified observable in collider physics.

Pythia Data

γ^*-decay events

Near the location of anticipated branch cuts, we see violent changes — a series of peaks and dips!

We can clearly see the discontinuity!

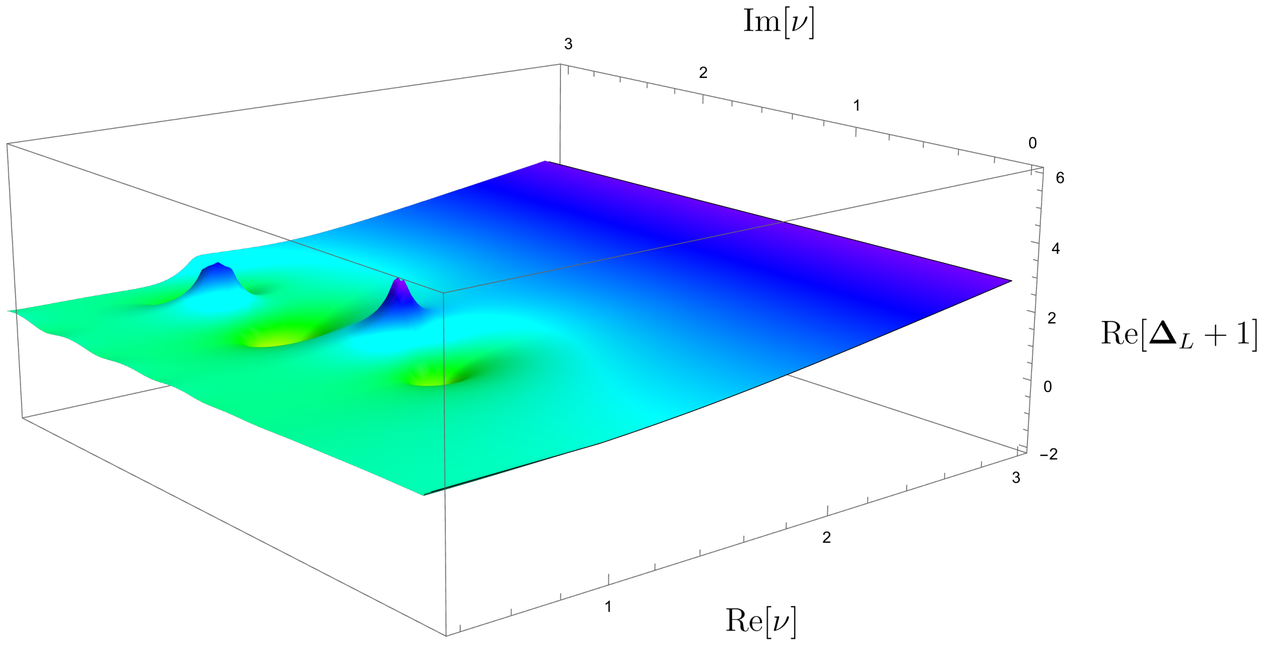

Real Part

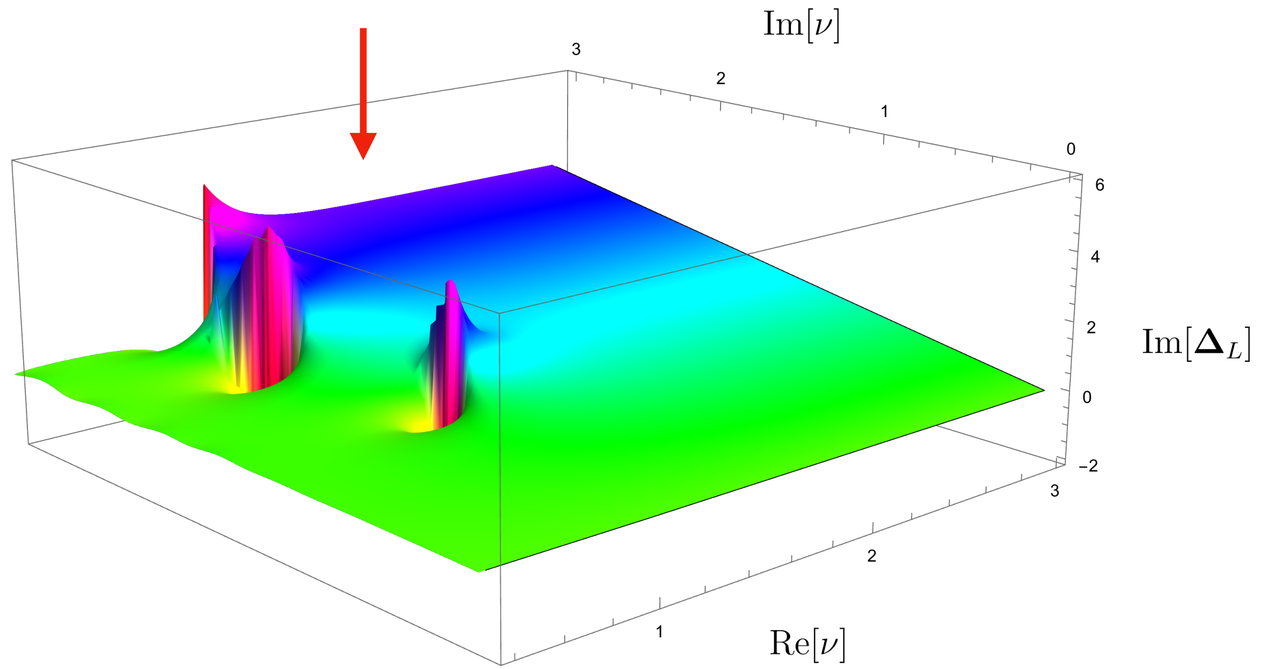

Imaginary Part

Pythia Data vs LO prediction

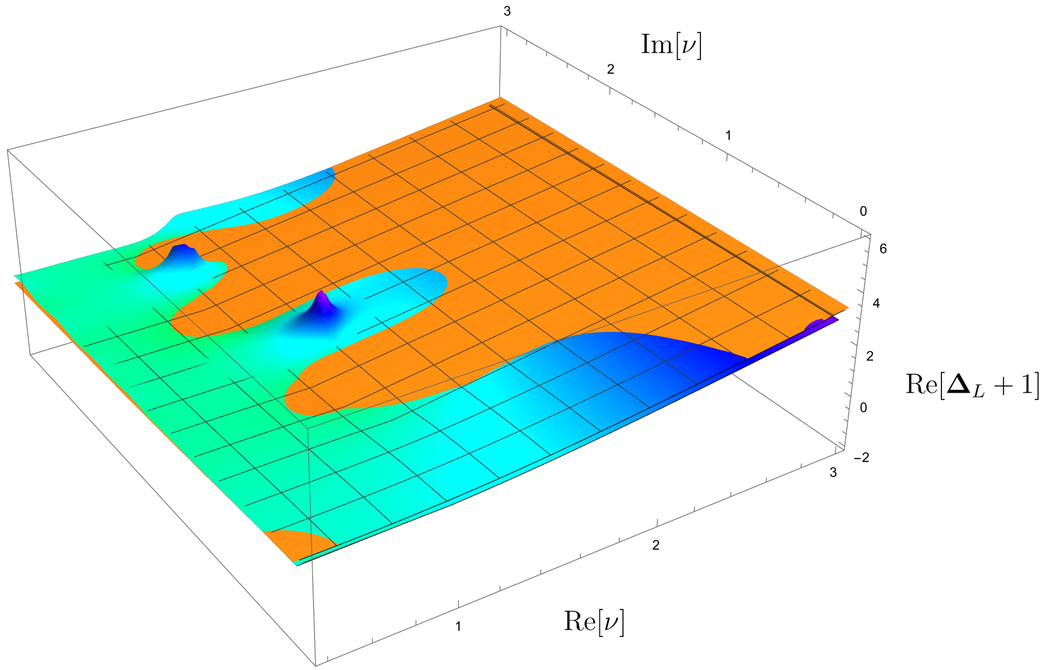

Real Part

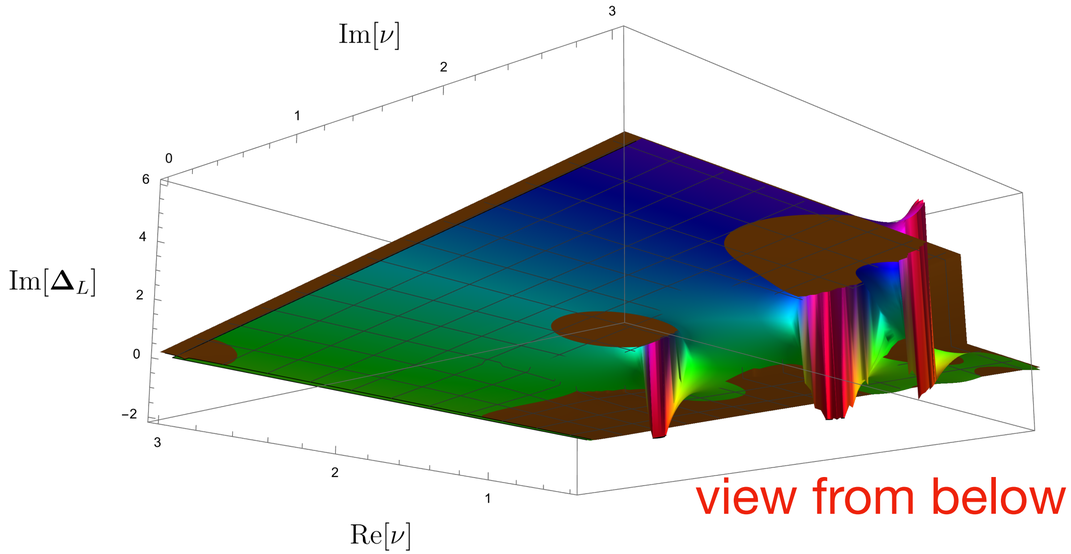

view from below

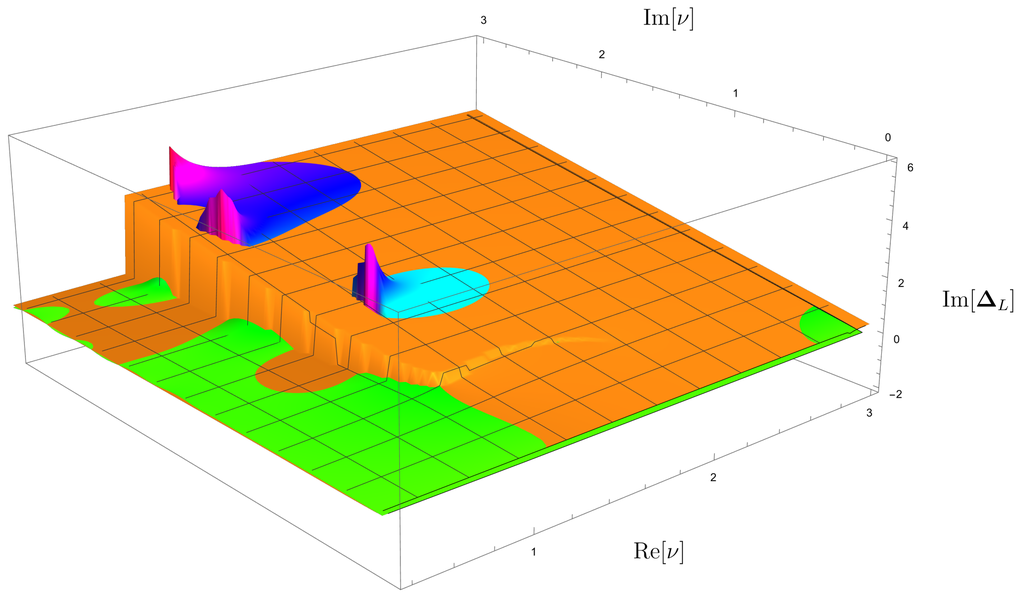

Imaginary Part

CMS Open Data

In complex space, the structure of branch cut seems to be robust to the effects of jet algorithms and other reasonable experimental cuts.

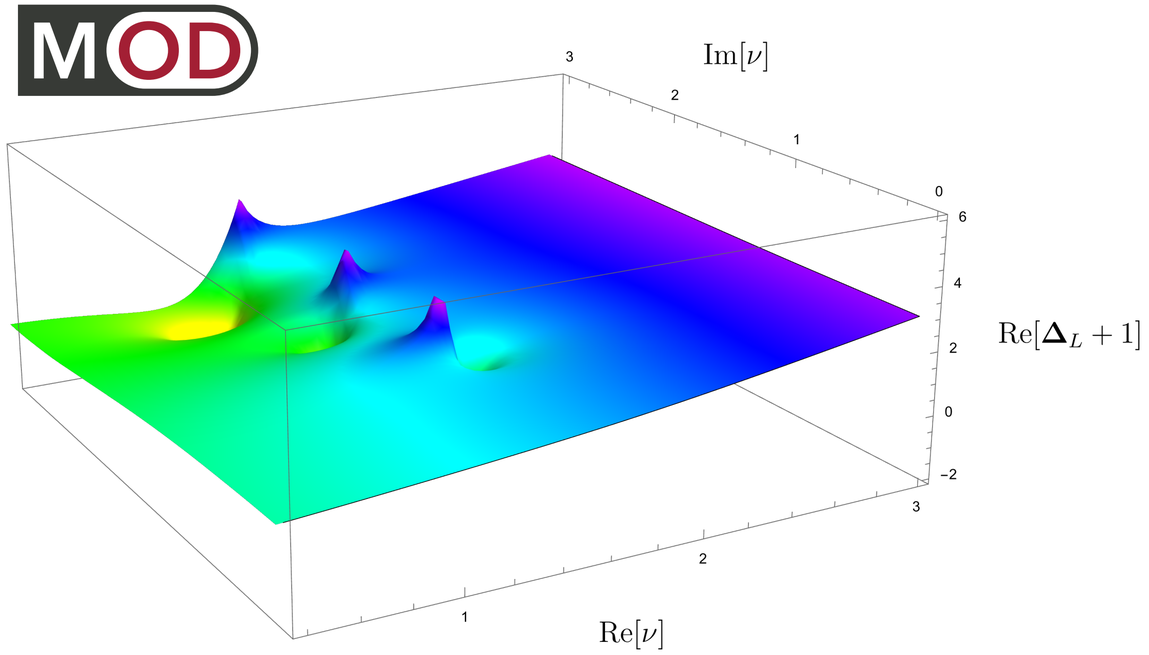

Real Part

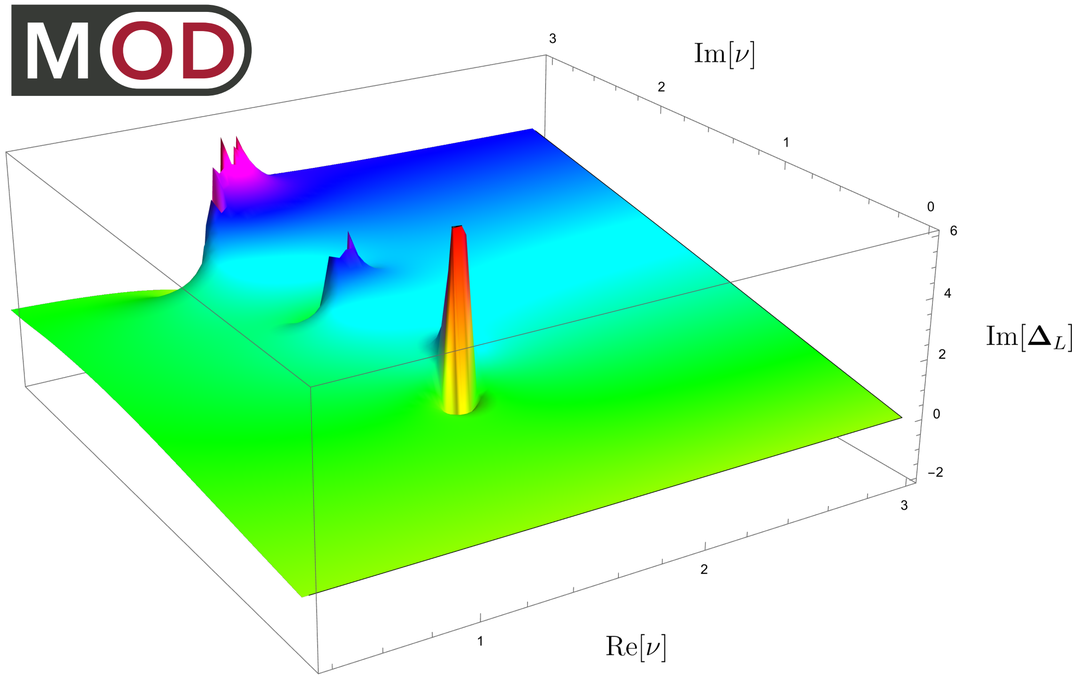

Imaginary Part

Behaviors Near Branch Cut

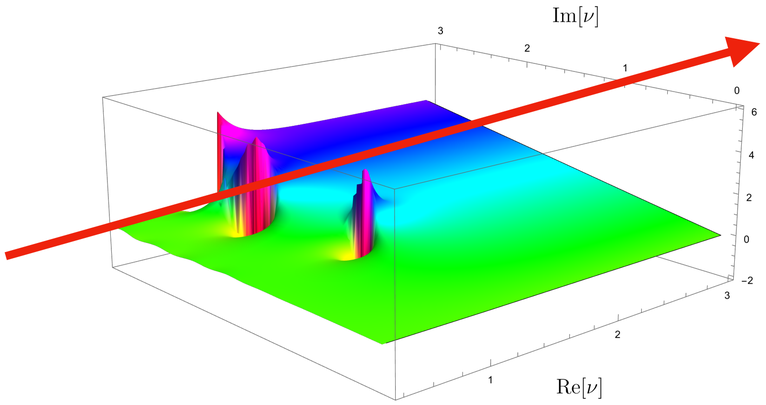

Choose a fixed $\mathrm{Im}\,\nu$ slice and
increase $\mathrm{Re}\,\nu$ to cross the branch cut

$x-$ axis: Q

$y-$ axis: $\ln(f(\nu, Q))$

- real part
- imaginary part

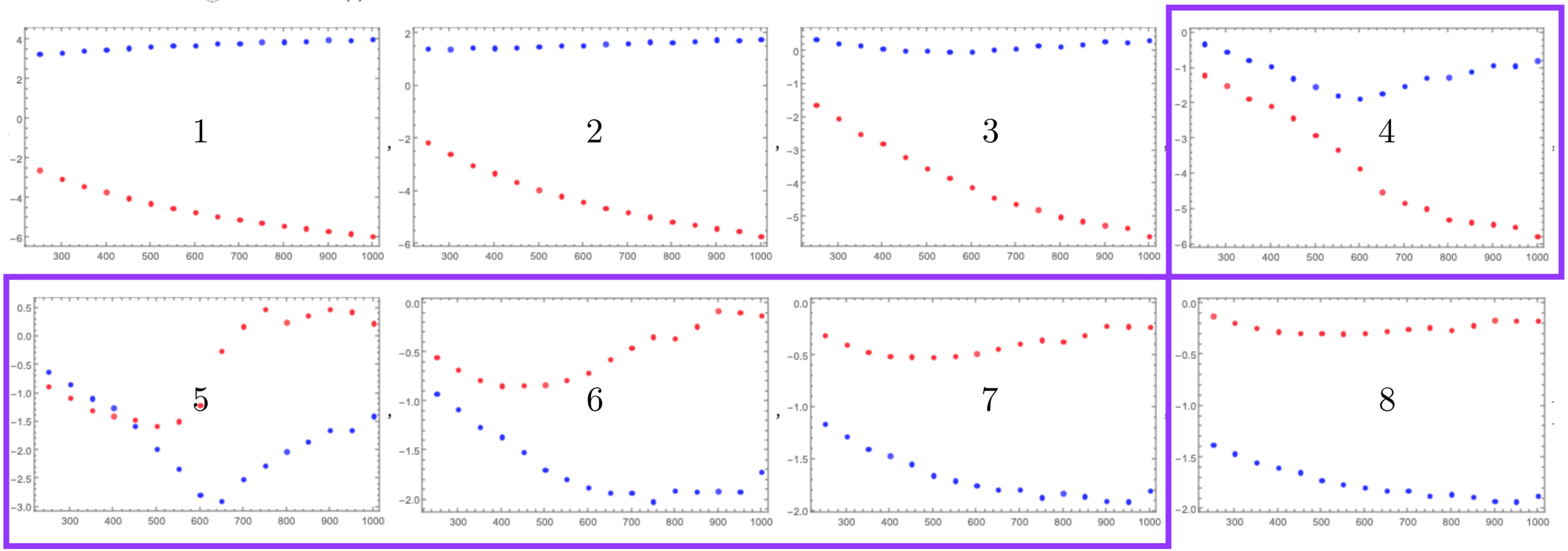

Near the branch cut, the ansatz $\ln(f) = \gamma \ln Q + c$ is not a good approximation

Q-evolution in the complex plane $f_\nu(Q) \equiv f(\nu, Q)$

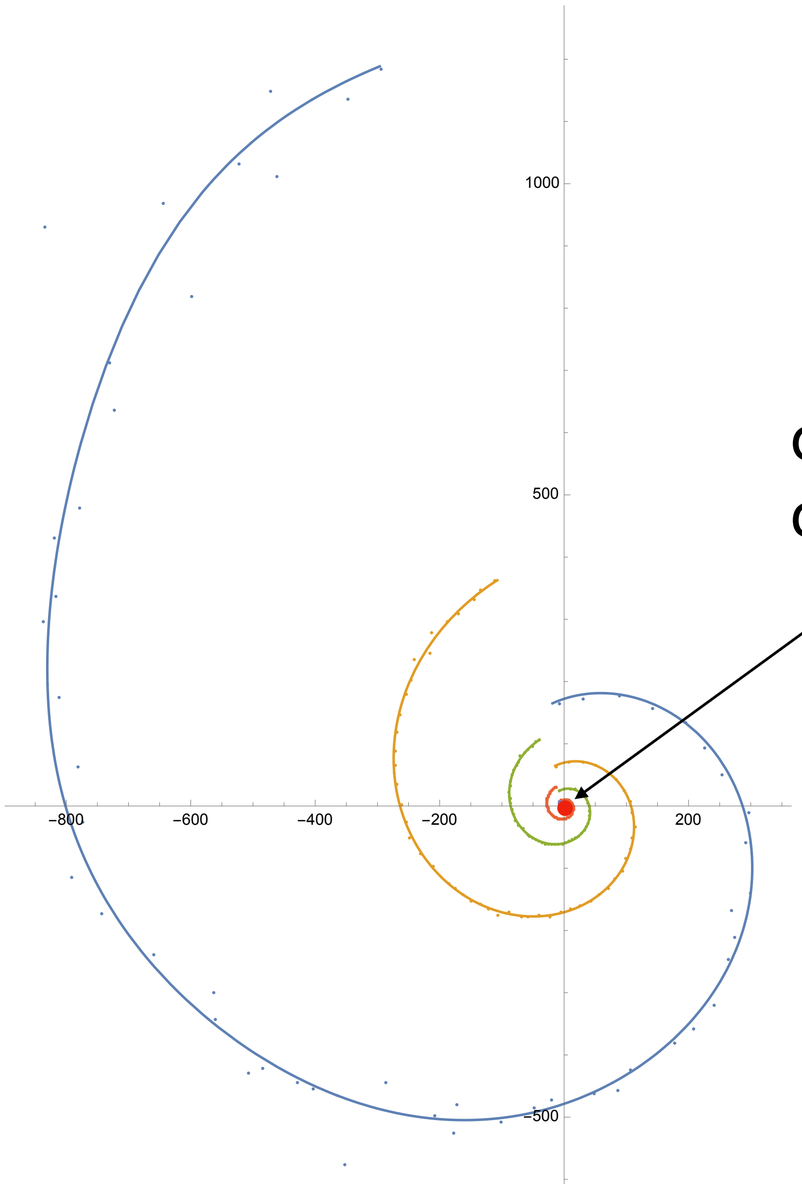

origin in the complex plane

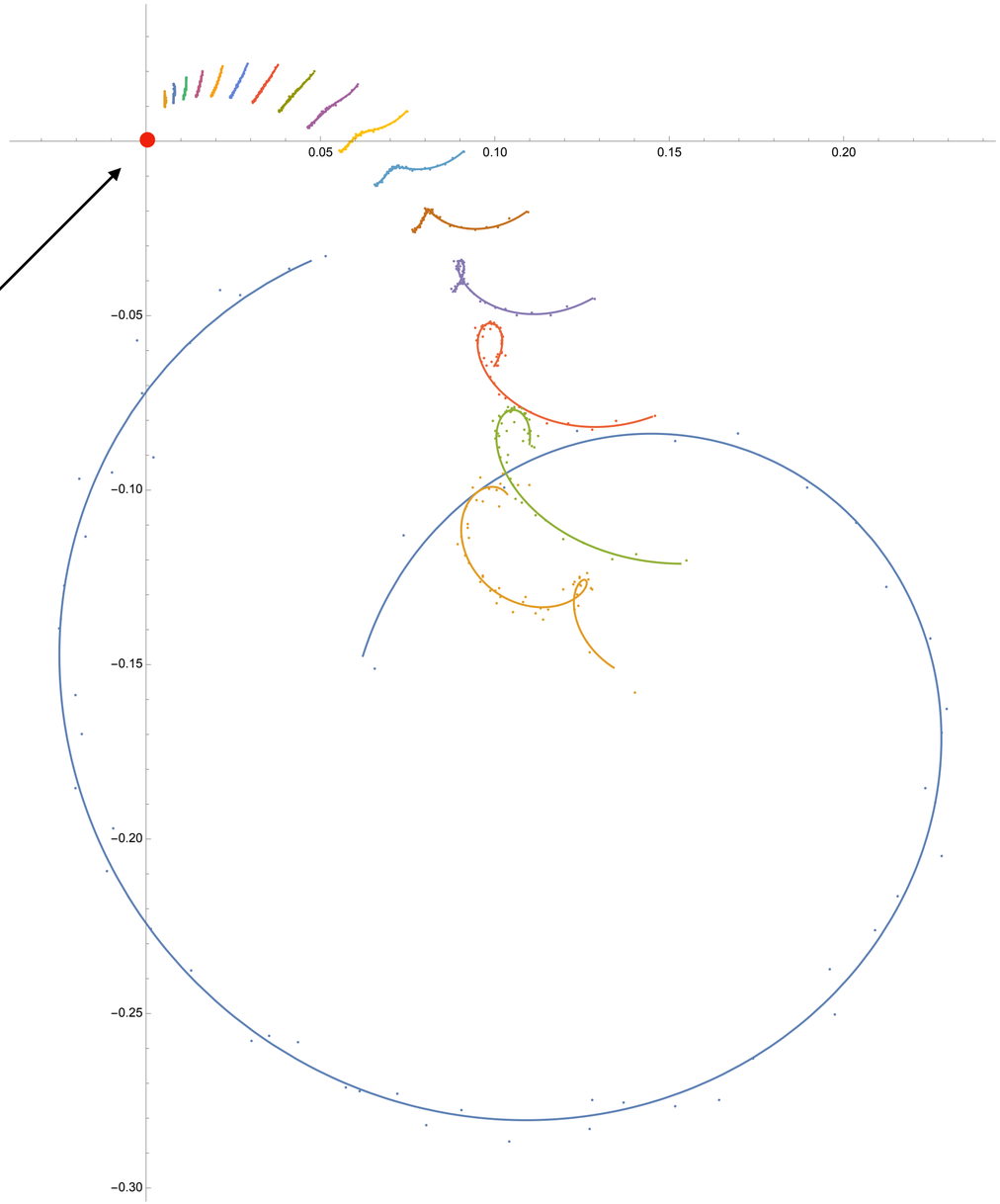

Q-evolution in the complex plane $f_\nu(Q) \equiv f(\nu, Q)$

On the LHS of the Branch Cut

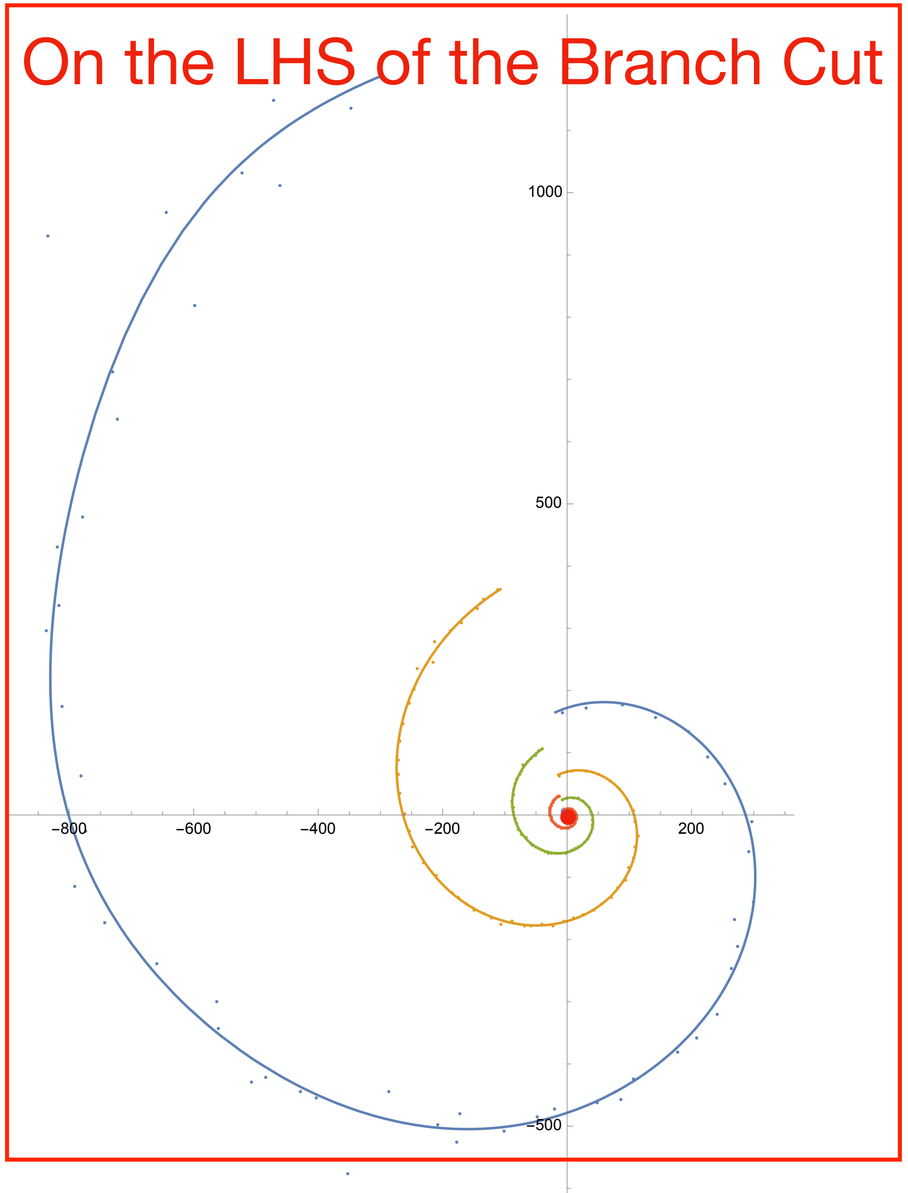

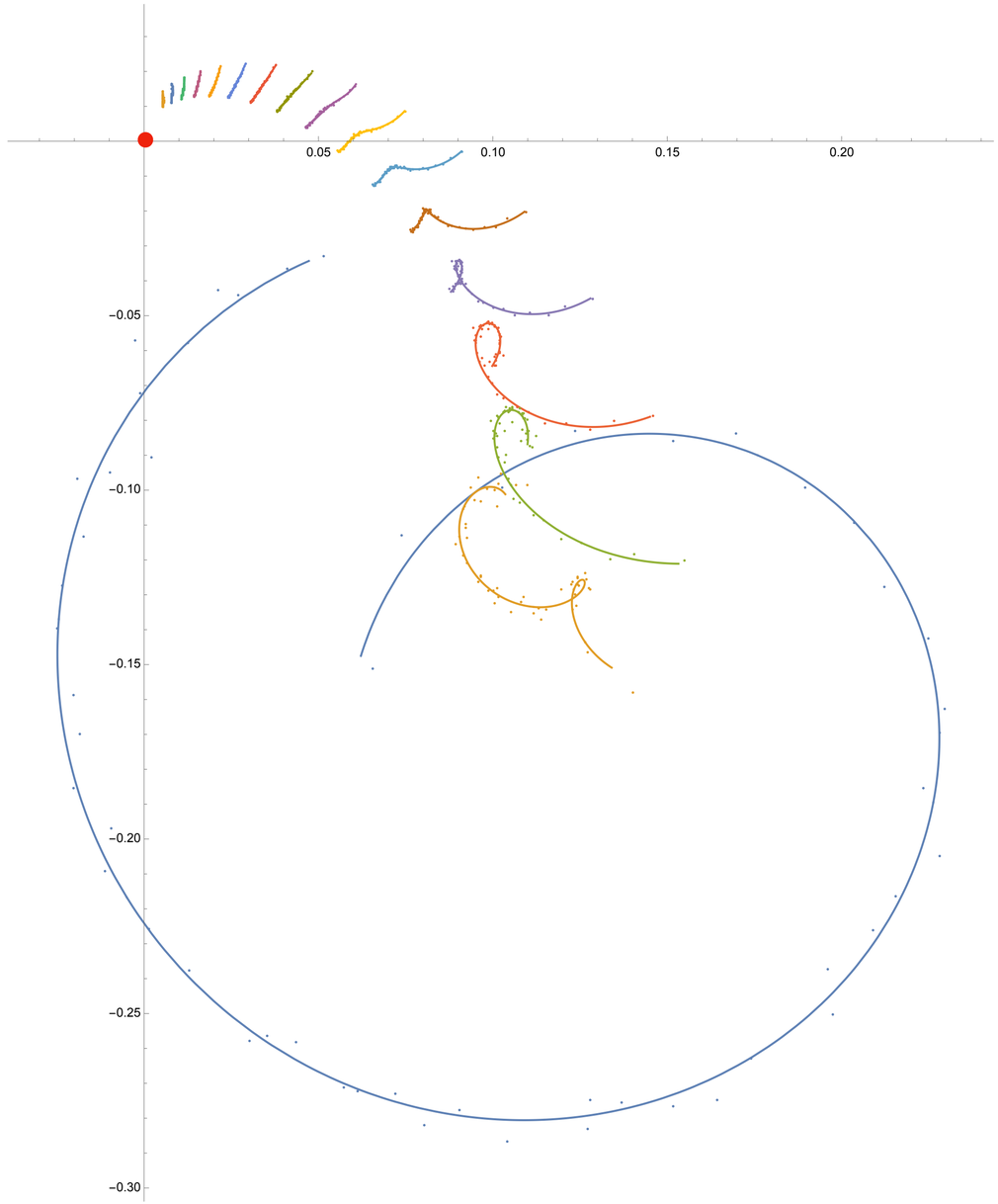

Q-evolution in the complex plane $f_\nu(Q) \equiv f(\nu, Q)$

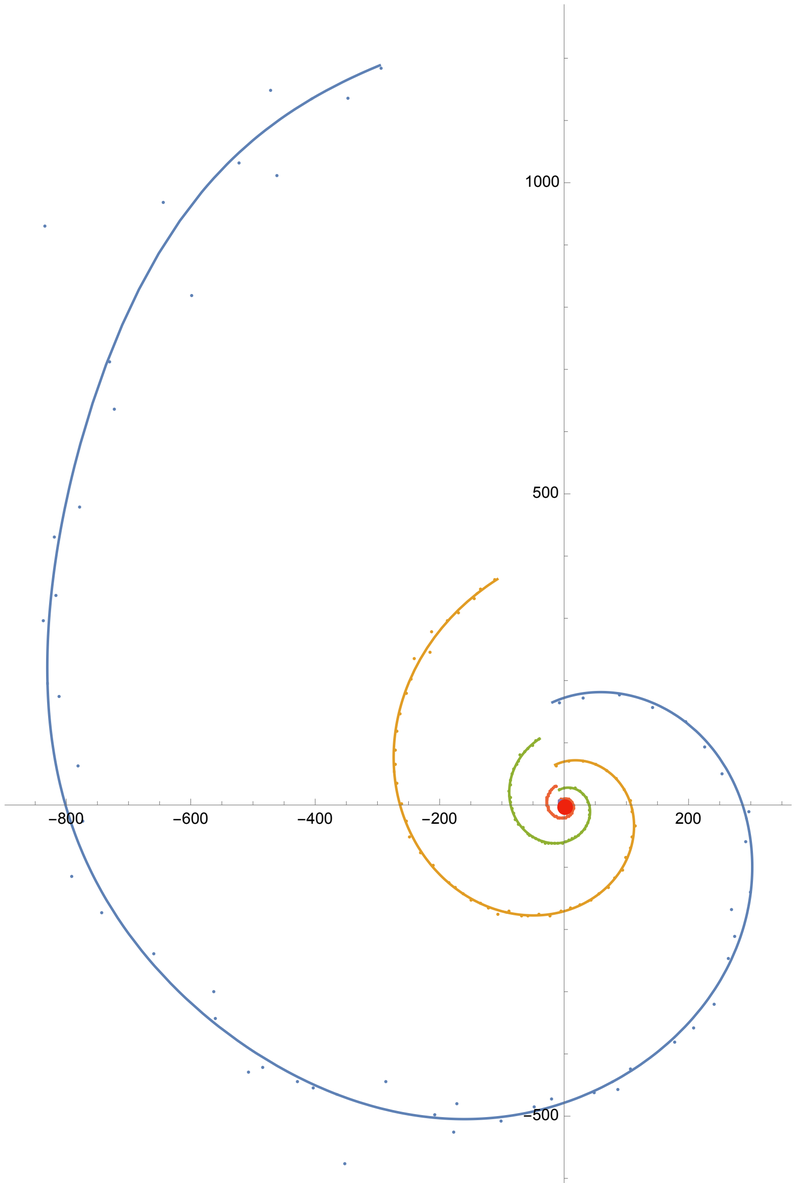

On the RHS of the Branch Cut

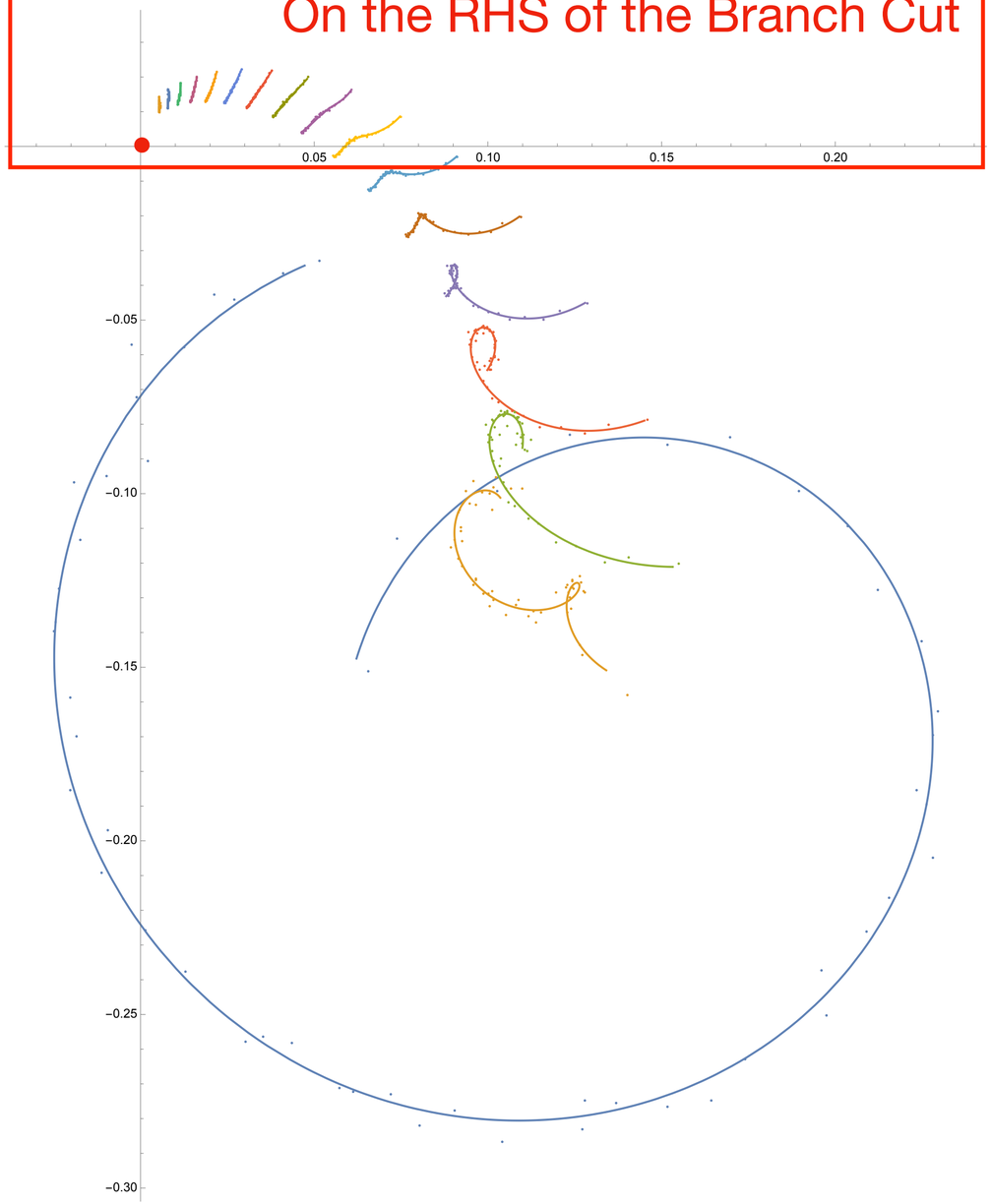

Q-evolution in the complex plane $f_\nu(Q) \equiv f(\nu, Q)$

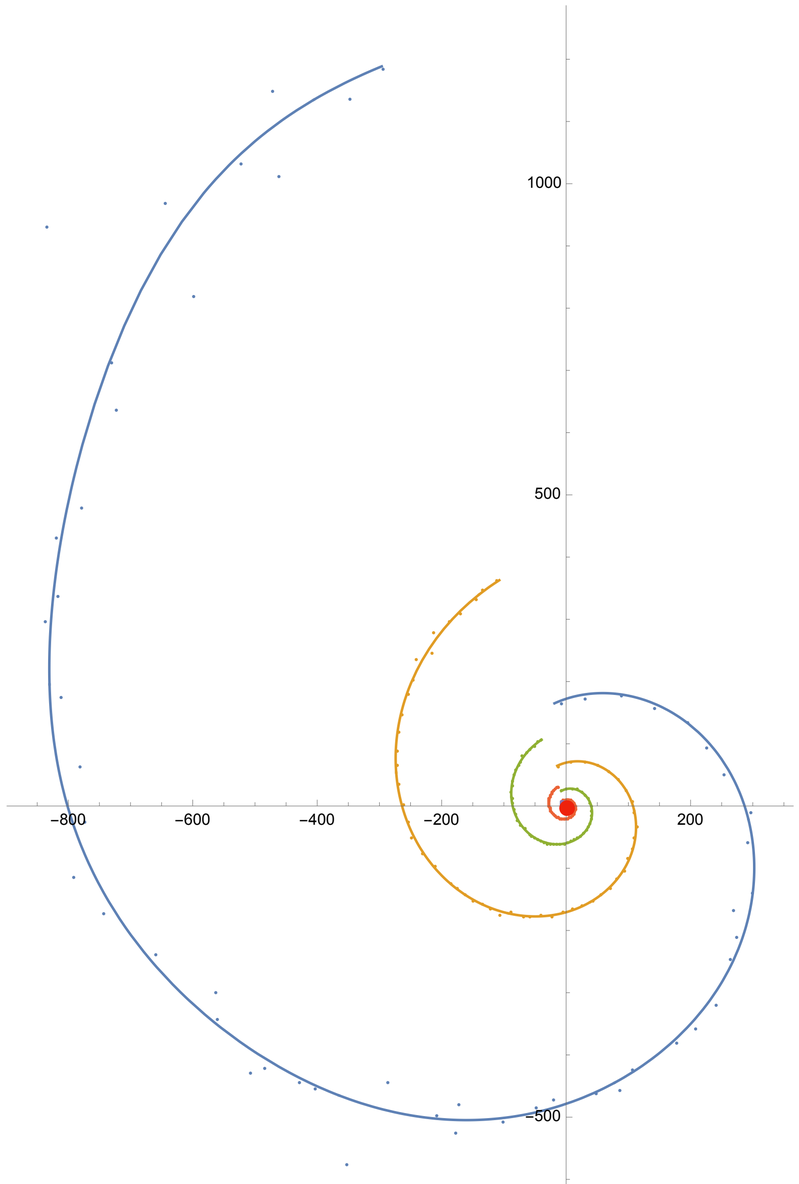

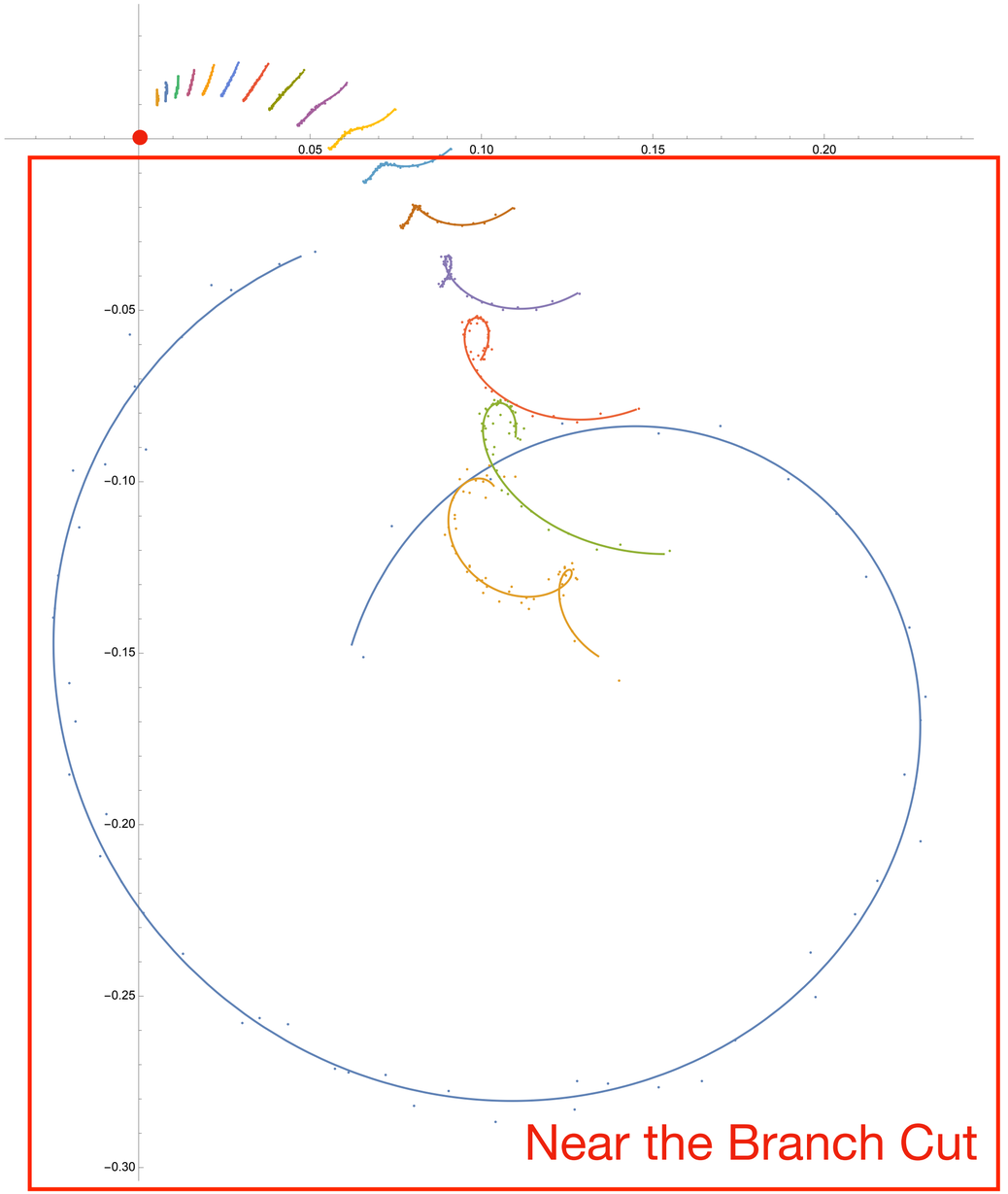

Q-evolution in the complex plane $f_\nu(Q) \equiv f(\nu, Q)$

Two competing evolution behaviors near the branch cut

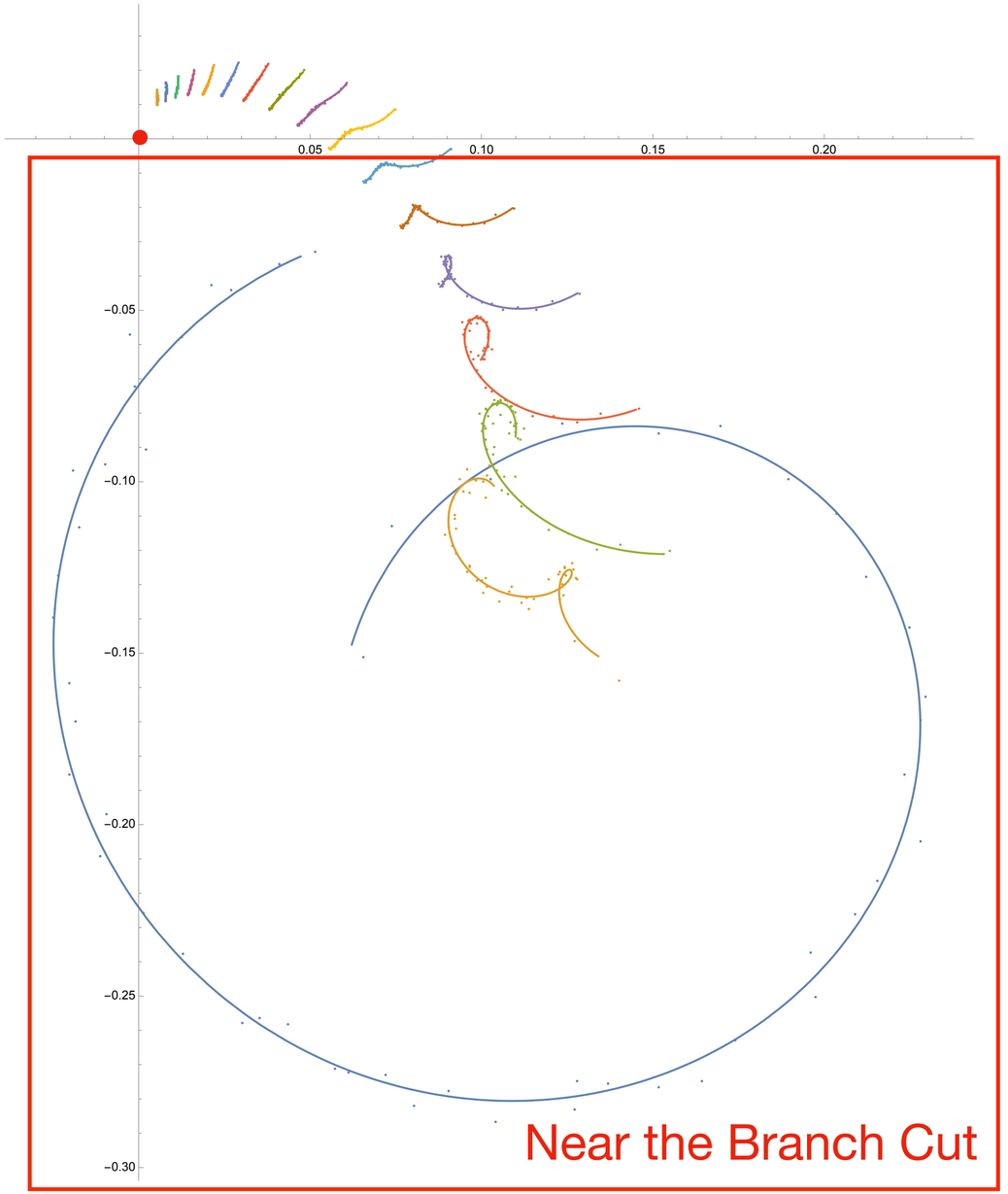

Near the Branch Cut

Two-Trajectory Approximation

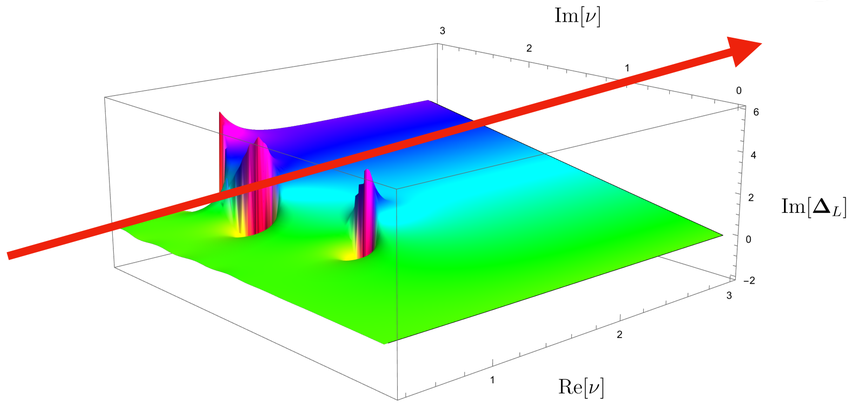

Near branch cut, the real part of two dimensions are very close

$$f = c_1 Q^{\gamma_1} + c_2 Q^{\gamma_2}$$

An example of two-trajectory fitting

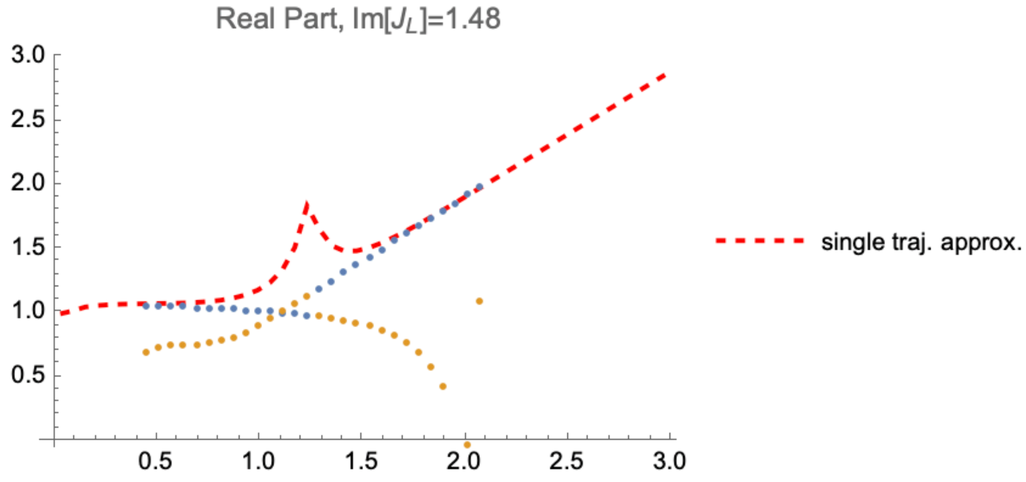

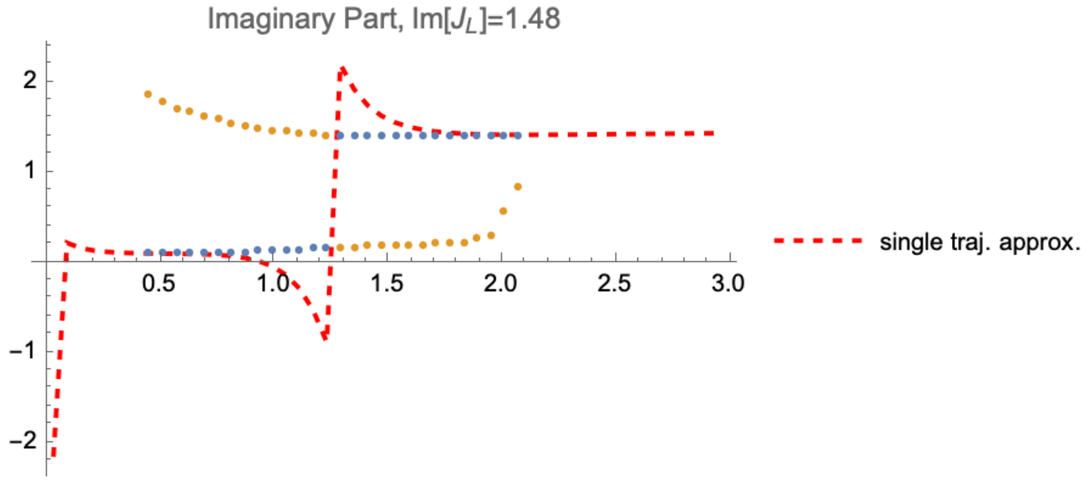

Two-Trajectory Approximation

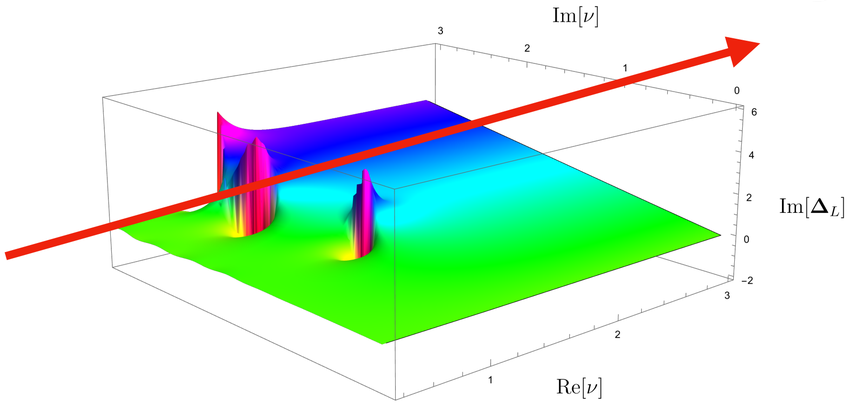

Near branch cut, the real part of two dimensions are very close

$$f = c_1 Q^{\gamma_1} + c_2 Q^{\gamma_2}$$

Preliminary result for two-trajectory fitting

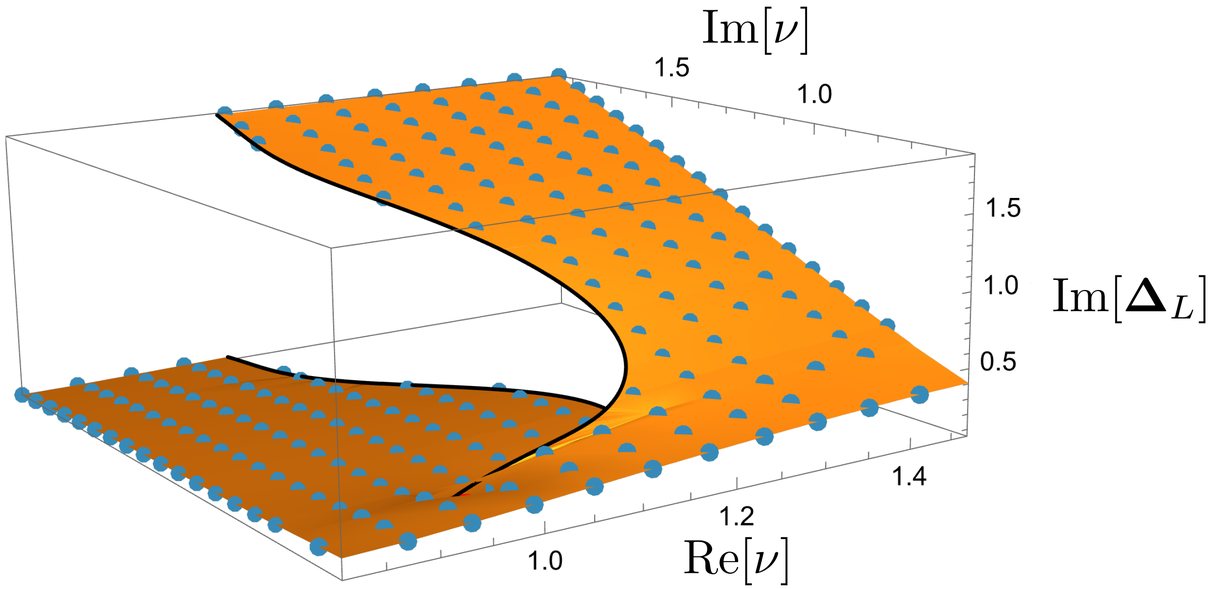

Other Application

CF Plot for Collinear Energy-Energy Correlator

Charged EEC @ LEP

Adapted from [2505.11828]

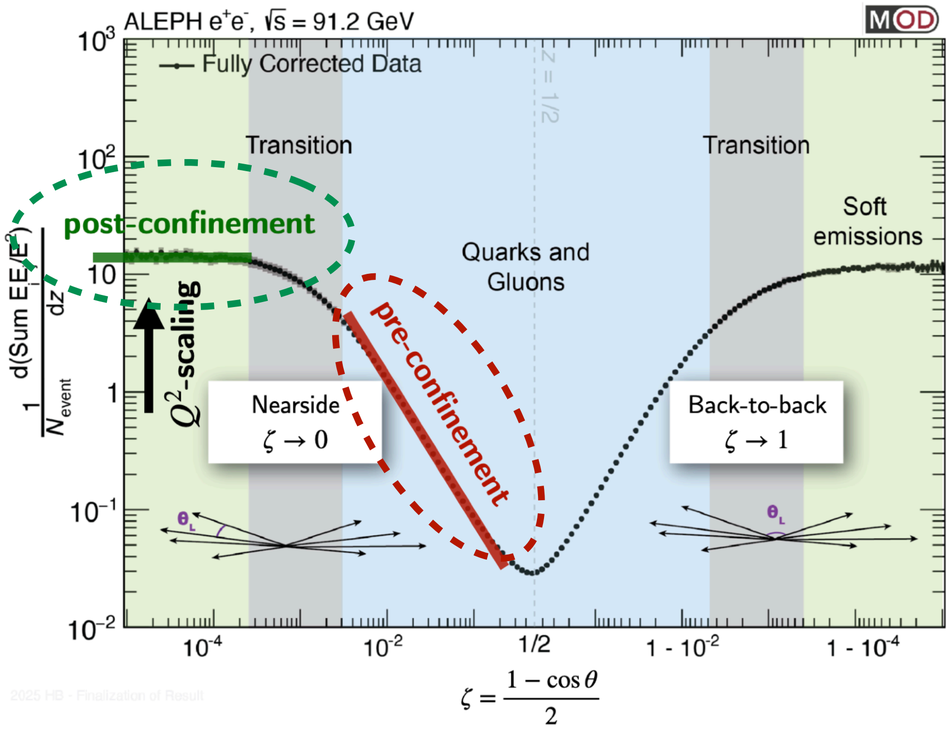

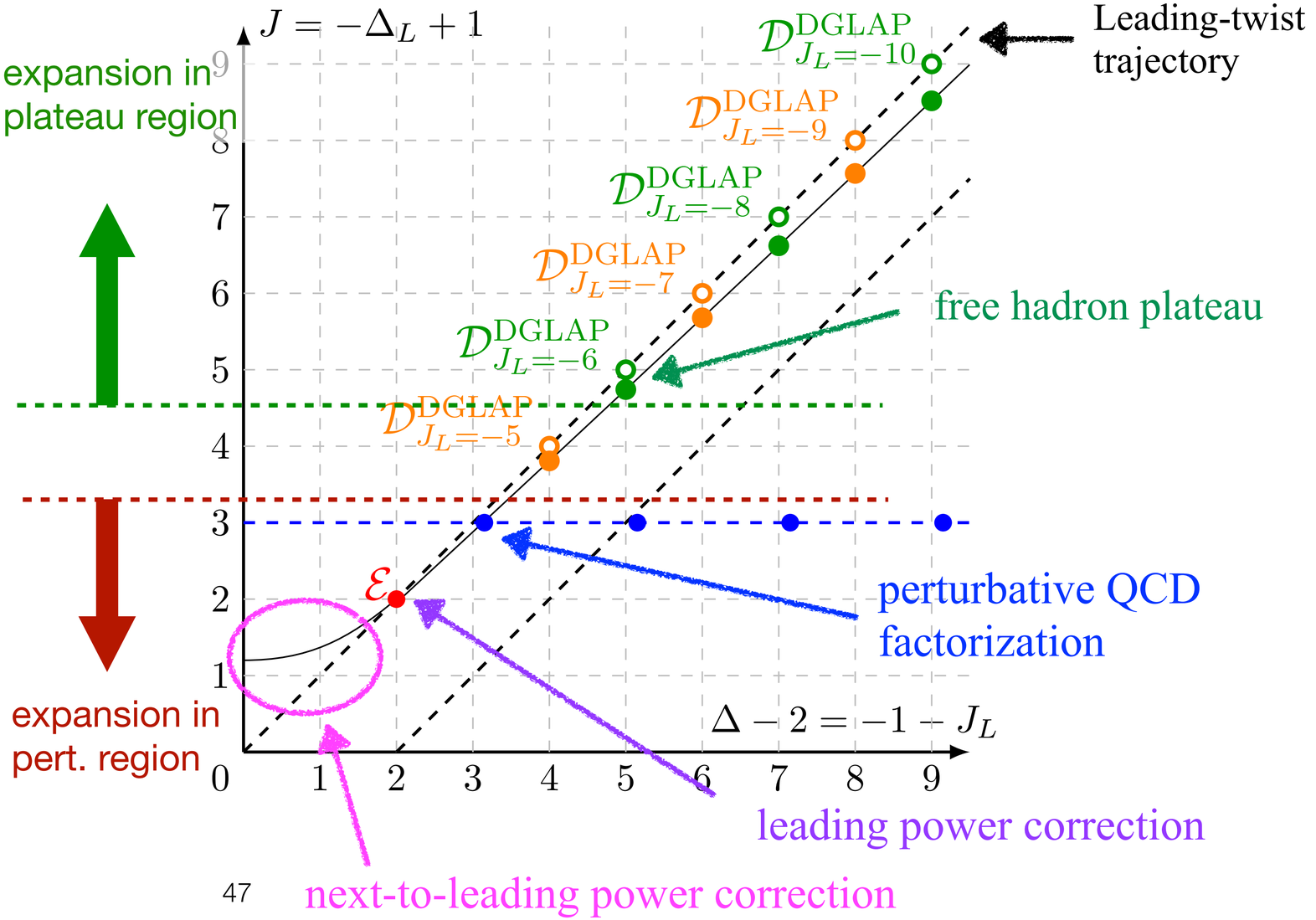

LP+NLP hadronization parametrization

Seems to be consistent with scale evolution of [hadron - parton] result in Pythia

Pythia γ^*/Z^*-decay

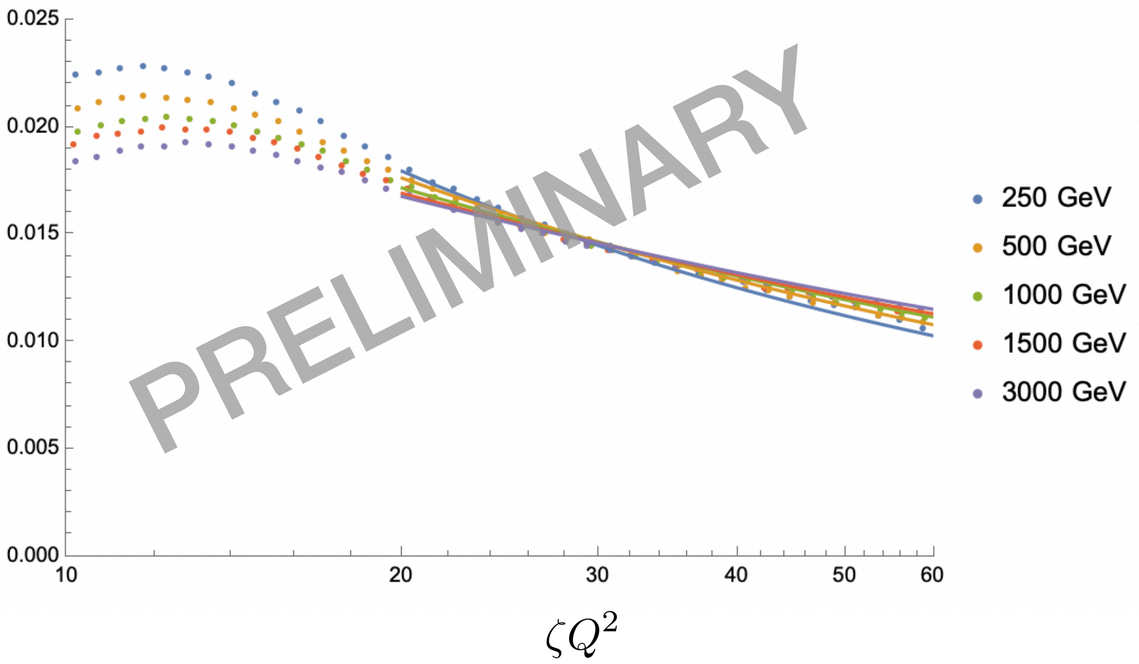

Pythia h^*-decay

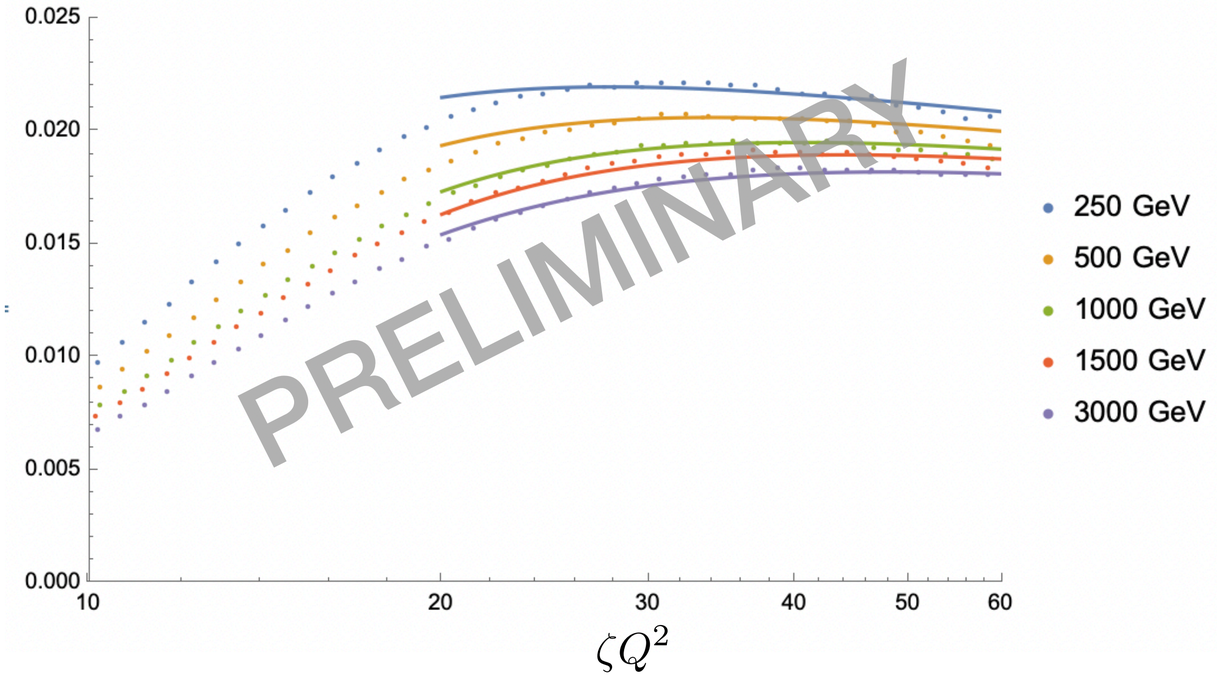

Caveat: too many non-perturbative parameters

light-ray operators
BFKL/DGLAP mixing

- renormalization
- level repulsion
- analyticity

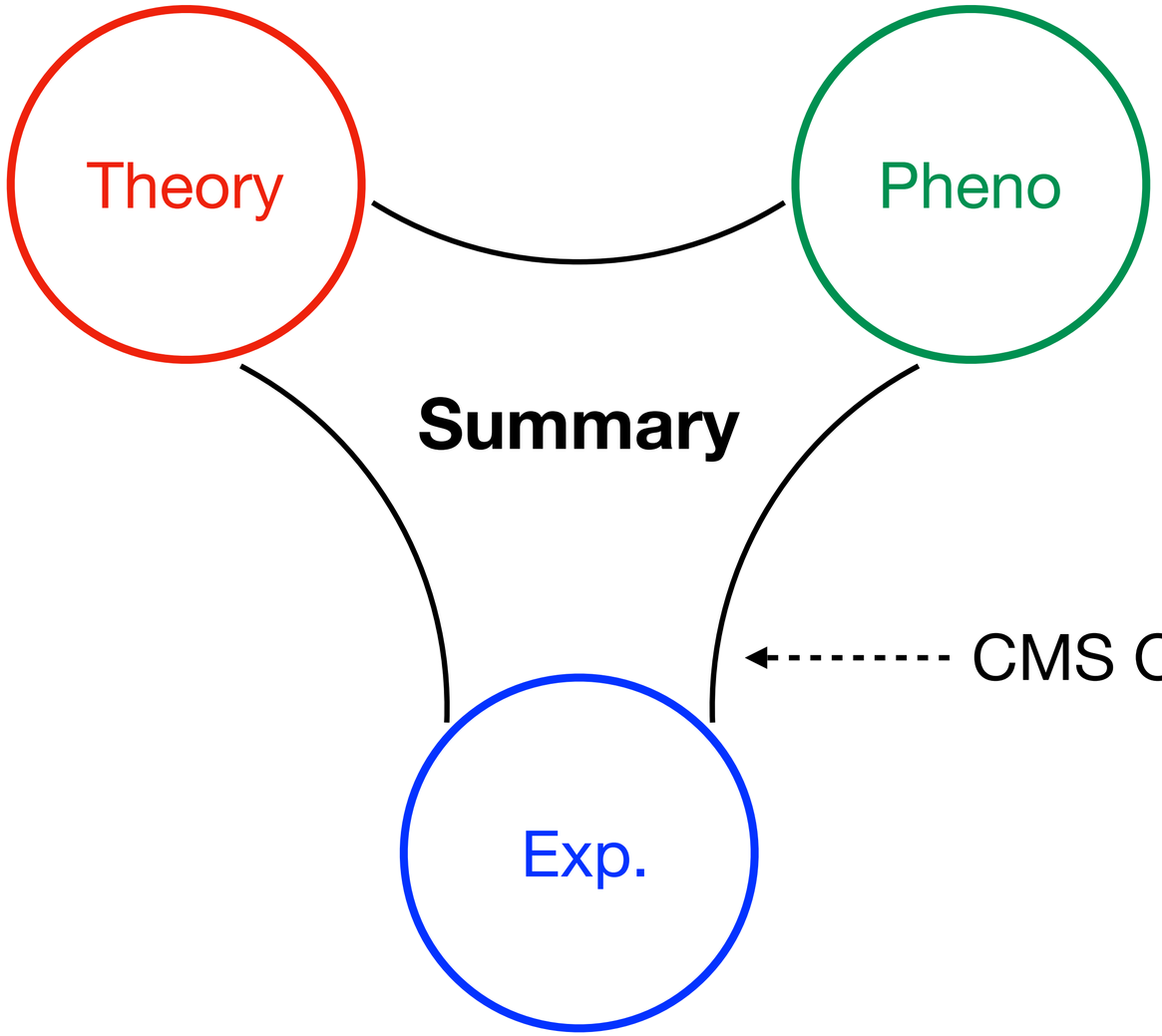

One-point event shape

- Factorization
- Complexification
- Pythia simulation

Thanks!

need our experimental colleagues

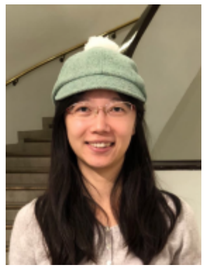

Meng Xiao